PHILOSOPHICAL TRANSACTIONS OF THE ROYAL SOCIETY A MATHEMATICAL, PHYSICAL & ENGINEERING SCIENCES

A Theory of a Broadening of the Infrared Absorption Spectra of Hydrogen-Bonded Species. III. The Kinematic and Electronic Coupling Mechanisms

G. N. Robertson

Phil. Trans. R. Soc. Lond. A 1977 **286**, 25-53
doi: 10.1098/rsta.1977.0109

Phil. Trans. R. Soc. Lond. A. **286**, 25–53 (1977) [25]
Printed in Great Britain

A THEORY OF A BROADENING OF THE INFRARED ABSORPTION SPECTRA OF HYDROGEN-BONDED SPECIES

III. THE KINEMATIC AND ELECTRONIC COUPLING MECHANISMS

By G. N. ROBERTSON
Department of Physics, University of Cape Town, Rondebosch, 7700, South Africa

(*Communicated by N. Sheppard, F.R.S. – Received 27 May 1976*)

CONTENTS

The theory of the coupling between anharmonic ν(XH) and ν(XH..Y) modes of a hydrogen-bonded complex developed in part II is extended so as to make explicit allowance for the effect of varying hydrogen bond length on the electron distribution of the XH molecule. Sufficient experimental data are available on the temperature dependence of the infrared spectrum of $Me_2O.HCl$ to enable the form of the potential energy surface to be deduced. The effective potential curves governing the hydrogen bond vibration in the ground and first excited state of the ν(XH) vibration are constructed. It is found that the $Me_2O.HCl$ complex is 14 pm shorter in the upper state than in the lower, which has important consequences for the structure of the vibration–rotation bands associated with vibrational Franck–Condon transitions. The shortening is much less pronounced in $Me_2O.DCl$.

The theory provides strong support for the interpretation of the broad ν(XH) bands of hydrogen bonded species in terms of ν(XH) $\pm n\nu$(XH..Y) combination bands, and demonstrates the close connection between the infrared spectroscopic anomalies and the Ubbelohde effect.

1. Introduction

In the two previous papers in this series (Coulson & Robertson 1974 and 1975, henceforth referred to as I and II) a theoretical basis was established for evaluating the contributions of vibrational predissociation and of combination band formation to the broadening of the infrared spectrum of a hydrogen-bonded species X—H..Y in the vapour phase. Numerical calculations for a linear triatomic model of the $Me_2O.HCl$ system showed that predissociation broadening is extremely unlikely to be observable, but that a kinematic coupling mechanism exists which necessarily leads to discernible combination band intensities. However, the experimental phenomena are more pronounced than those calculated in II, and this suggests that an additional coupling mechanism may be operative.

In both these papers a very simple model potential energy surface was used, namely

$$V(r, R) = V_1(r) + V_2(R), \tag{1.1.1}$$

where $V_1(r)$is either a harmonic or an anharmonic oscillator potential in the XH bond length r and $V_2(R)$ is a Morse function in the H..Y bond length R. This assumes tacitly that the XH interaction is unaffected by hydrogen bond formation and is independent of hydrogen bond length.

It is, however, well known that with decreasing hydrogen bond length there is a progressive shift of the ν(XH) absorption towards lower frequencies (Sheppard 1959), and this suggests strongly that a more accurate representation of the potential energy surface would allow for a reduction in the curvature of $V(r, R)$, considered as a function of r, as R is decreased. This can be accomplished formally by writing

$$V(r, R) = V_1(r) + V_2(R) + V_3(r, R), \tag{1.1.2}$$

where $V_1(r)$ and $V_2(R)$ are as before, $V_3(r, \infty)$ vanishes, and $\partial^2/\partial r^2 V_3(r, R)$ is negative near the hydrogen bond equilibrium position (r_0, R_0). The addition of the term $V_3(r, R)$ will further couple the two stretching modes as well as leading to a downward shift in the ν(XH) absorption frequency. Since the term reflects the change in the electron distribution in the XH molecule associated with hydrogen bond formation, it seems natural to refer to its effect on the vibrational dynamics as an electronic coupling mechanism.

Little information is available about the nature of the term $V_3(r, R)$, and it is necessary to assume a particular functional form. For analytical convenience $V_3(r, R)$ will be taken as the product of $V_1(r)$ and a modulating factor which depends on the hydrogen bond length and on two fixed parameters.† This choice enables effective potential curves governing the ν(XH..Y) vibration in the ground and first excited state of the ν(XH) vibration to be derived by a straightforward extension of the method of II. The intensities of the transitions $|0, n_0\rangle \rightarrow |1, n_1\rangle$ can then be calculated in terms of vibrational Franck–Condon factors and Boltzmann factors in essentially the same way as before.

Inclusion of the term $V_3(r, R)$ allows a much better reconstruction of the infrared spectrum of $Me_2O.HCl$ to be effected. Although one of the parameters characterizing the potential energy surface cannot be derived directly from experimental data, the temperature dependence of the reconstructed spectrum is found to be sensitive to variations in this parameter. A good deal of experimental information on the temperature dependence of the spectrum of $Me_2O.HCl$ is available (Lassègues & Huong 1972; Bertie & Falk 1973). By choosing the undetermined

† This is very similar to the coupling term used by Witkowski & Y. Maréchal (1968).

parameter so as best to reproduce this temperature dependence it is possible to obtain fairly reliable information about the potential energy surface near its global minimum. However, it has to be assumed that electrical anharmonicity does not contribute to the intensities of Franck–Condon transitions.

An important feature of the more realistic potential energy surface is that it predicts both effective potential curves for the ν(XH . . Y) vibration to be displaced towards smaller values of the coordinate, in contrast to the results of II. The displacement is much greater for the upper than for the lower curve, and in each case it is reduced by deuterium substitution. It follows that the hydrogen bond in Me_2O . HCl is considerably shorter in the first excited ν(XH) state than in the ground state, and that it is somewhat shorter in the protium than in the deuterium species.

This has three main consequences. First, it implies that the widths of $|1, n_1\rangle$ levels calculated in I are rather too small. Secondly, it means that the moment of inertia of the complex will be appreciably smaller in the first excited ν(XH) vibrational state than in the ground state, which will result in every $|0, n_0\rangle \rightarrow |1, n_1\rangle$ transition having an anomalous rotational fine structure, similar to that observed in the CH_3CN . HCl spectrum by Thomas & Thompson (1970). Finally, the reduction in the separation between the minima of the curves produced by deuterium substitution will affect both the vibrational Franck–Condon factors and the rotational fine structure of the spectrum. This is closely connected with the normal Ubbelohde effect in solids, i.e. with the lattice expansion of a hydrogen-bonded crystal on deuteration (Ubbelohde 1939).

The main purpose of this paper is to show that many of the observed features of the spectrum of Me_2O . HCl in the vapour phase can be understood in terms of the anharmonic coupling between ν(XH) and ν(XH . . Y) stretching modes and the consequent vibration–rotation interaction. Other effects which may influence the observed spectrum include electrical anharmonicity and the excitation of combinations involving hydrogen bond bending modes. Although it is impossible at this stage to judge whether the former is of practical importance, it seems likely that the latter plays a significant rôle.

2. Theory of combination band formation

2.1. *The model potential energy surface*

The analysis of § 2 of II needs only minor modification in order to accommodate a potential energy surface of form (1.1.2). It is again convenient to use a Jacobi coordinate system in which the hydrogen bond length R is eliminated in favour of a coordinate s defined by

$$s = \gamma r + R, \tag{2.1.1}$$

where

$$\gamma = m_X/(m_X + m_H). \tag{2.1.2}$$

This enables the centre-of-mass motion to be separated off immediately, while diagonalizing the kinetic energy matrix in the internal coordinates r and s. The model potential energy surface will be chosen as

$$V(r, s) = V_1(r) + V_2(R) + V_3(r, s), \tag{2.1.3}$$

where

$$V_1(r) = D_1(1 - e^{-\beta(r-r_0)})^2 \tag{2.1.4}$$

$$V_2(R) = D_2(-2e^{-\alpha(R-R_0)} + e^{-2\alpha(R-R_0)}) \tag{2.1.5}$$

and

$$V_3(r, s) = (c_1 e^{-\alpha(s-s_0)} + c_2 e^{-2\alpha(s-s_0)}) V_1(r). \tag{2.1.6}$$

$V_1(r)$ and $V_2(R)$ are as used in II, and the dissociation energies and Morse exponents can be determined from experimental data in the same way as before. The form of the term $V_3(r, s)$ is chosen primarily for analytical convenience. The main advantage of this choice is that it allows very simple expressions to be obtained for the potential energy curves describing the ν(XH..Y) motion, irrespective of the values of the two parameters c_1 and c_2, while affording considerable flexibility. If the sum of c_1 and c_2 is negative, the second derivative $\partial^2/\partial r^2\, V_3(r, s)$ will be smaller near the global minimum (r_0, s_0) of the potential energy surface than at (r_0, ∞), and this makes provision for the effect on the ν(XH) vibration of variations in hydrogen bond length, i.e. for the electronic coupling effect. A kinematic coupling mechanism is also operative, as before, owing to the dependence of $V_2(R)$ on r when the internal coordinate s of (2.1.1) is used.

The hamiltonian governing the vibrational motion becomes

$$\hat{H} = -\frac{\hbar^2}{2\mu_1}\frac{\partial^2}{\partial r^2} - \frac{\hbar^2}{2\mu_2}\frac{\partial^2}{\partial s^2} + D_1\left(1 + c_1 e^{-\alpha(s-s_0)} + c_2 e^{-2\alpha(s-s_0)}\right)\left(1 - e^{-\beta(r-r_0)}\right)^2 + D_2\left[-2e^{-\alpha(s-s_0)-\gamma(r-r_0))} + e^{-2\alpha(s-s_0)-\gamma(r-r_0))}\right], \quad (2.1.7)$$

the reduced masses being given by

$$\mu_1^{-1} = m_X^{-1} + m_H^{-1} \quad (2.1.8)$$

and

$$\mu_2^{-1} = (m_X + m_H)^{-1} + m_Y^{-1}. \quad (2.1.9)$$

By appeal to the adiabatic separability of the two vibrational modes, an approximate solution to the Schrödinger equation

$$\hat{H}\Psi(r, s) = E\Psi(r, s) \quad (2.1.10)$$

may be sought in the form

$$\Psi_{m,n}(r, s) = \chi_m(r)\, g_{m,n}(s), \quad (2.1.11)$$

where

$$\{\hat{T}_r + V_1(r) + V_3(r, s_0)\}\chi_m(r) = \epsilon_m \chi_m(r). \quad (2.1.12)$$

The functions $g_{0,n}(s)$ and $g_{1,n}(s)$ describe the nth bound state of the ν(XH..Y) vibration in the ground and first excited state of the ν(XH) motion. After substituting (2.1.11) in (2.1.7), pre-multiplying by $\chi_m(r)$, and integrating over r, it is found that the $g_{m,n}(s)$ satisfy

$$\left[\frac{d^2}{ds^2} - \frac{2\mu_2}{\hbar^2}\left\{\epsilon_m - E_{m\ n} + \int_0^\infty \chi_m(r)\left[V_2(s-\gamma r) + V_3(r, s) - V_3(r, s_0)\right]\chi_m(r)\, dr\right\}\right] g_{m,n}(s) = 0. \quad (2.1.13)$$

It is convenient to define

$$U_{mm}(s) = \frac{2\mu_2}{\hbar^2}\int_0^\infty \chi_m(r)\left[V_2(s-\gamma r) + V_3(r, s)\right]\chi_m(r)\, dr \quad (2.1.14)$$

and

$$\Delta\epsilon_m = -\int_0^\infty \chi_m(r)\, V_3(r, s_0)\, \chi_m(r)\, dr, \quad (2.1.15)$$

whereupon (2.1.13) can be written

$$\left[\frac{d^2}{ds^2} - U_{mm}(s) - \frac{2\mu_2}{\hbar^2}(\epsilon_m + \Delta\epsilon_m - E_{m,n})\right] g_{m,n}(s) = 0. \quad (2.1.16)$$

Comparison with equations (2.1.8), (2.1.12) and (2.1.13) of II shows that the effect of the additional coupling term $V_3(r, s)$ is to change the definition of the effective potential curve $U_{mm}(s)$ which governs the hydrogen bond vibration in the mth state of the ν(XH) vibration, to change the definition of ϵ_m, and to produce a further level shift $\Delta\epsilon_m$.

From (2.1.5) and (2.1.6) it follows that

$$U_{mm}(s) = \frac{2\mu_2 D_2}{\hbar^2}\{-2a_{mm}\,\mathrm{e}^{-\alpha(s-s_0)} + b_{mm}\,\mathrm{e}^{-2\alpha(s-s_0)}\}, \tag{2.1.17}$$

where

$$a_{mm} = \int_0^\infty \chi_m(r)\left\{\mathrm{e}^{\alpha\gamma(r-r_0)} - \frac{c_1 D_1}{2D_2}(1-\mathrm{e}^{-\beta(r-r_0)})^2\right\}\chi_m(r)\,\mathrm{d}r \tag{2.1.18}$$

and

$$b_{mm} = \int_0^\infty \chi_m(r)\left\{\mathrm{e}^{2\alpha\gamma(r-r_0)} + \frac{c_2 D_1}{D_2}(1-\mathrm{e}^{-\beta(r-r_0)})^2\right\}\chi_m(r)\,\mathrm{d}r. \tag{2.1.19}$$

The purpose of the somewhat artificial choice of $V_3(r, R)$ is now clear: with this form of function the effective potential curves $U_{00}(s)$ and $U_{11}(s)$ governing the ν(XH..Y) vibration remain Morse functions, but have shifted minima and altered depths. These are given by

$$s_{mm} = s_0 + \alpha^{-1}\ln(b_{mm}/a_{mm}), \tag{2.1.20}$$

and

$$D_{mm} = D_2(a_{mm}^2/b_{mm}). \tag{2.1.21}$$

As is seen from (2.1.18) and (2.1.19), both the kinematic and the electronic coupling mechanisms affect the values of the coefficients a_{mm} and b_{mm} in terms of which the displacement along the abscissa, the curvature near the minimum, and the overall depth of the potential functions $U_{00}(s)$ and $U_{11}(s)$ are determined.

2.2. *The* ν(XH..Y) *vibrational wave functions*

Apart from the differences in the definition of the a_{mm} and b_{mm}, equation (2.1.17) above is identical with (2.2.21) of II, and the analysis of §§ 2.2 and 2.3 of that paper can now be used with very little modification. By defining

$$z = \exp(-\alpha(s-s_0)) \tag{2.2.1}$$

$$\tau = (2\mu_2 D_2)^{\frac{1}{2}}/\alpha\hbar \tag{2.2.2}$$

and

$$q_m = \tau a_{mm}/b_{mm}^{\frac{1}{2}}, \tag{2.2.3}$$

it is possible to transform (2.1.16) into the standard form of Whittaker's confluent hypergeometric equation (Whittaker & Watson 1927). It can hence be shown that the eigenfunctions for the ν(XH..Y) vibration are given by

$$g_{m,n}(s) = N_{mn}\,z^{-\frac{1}{2}}M_{q_m, q_m-n-\frac{1}{2}}(2\tau b_{mm}^{\frac{1}{2}}z), \tag{2.2.4}$$

where M denotes the Whittaker function which is regular at the origin, and N_{mn} is a normalizing constant. The energies of $|m, n\rangle$ states are given by

$$E_{m,n} = \epsilon_m + \Delta\epsilon_m - D_2(q_m - n - \tfrac{1}{2})^2/\tau^2. \tag{2.2.5}$$

The Franck–Condon factor governing the intensity of $|0, n_0\rangle \rightarrow |1, n_1\rangle$ transitions is the square of the overlap integral c_{n_0, n_1}, where

$$\begin{aligned} c_{n_0,n_1} &= \int_0^\infty g_{1,n_1}(s)\,g_{0,n_0}(s)\,\mathrm{d}s \\ &= N_{1,n_1}N_{0,n_0}\alpha^{-1}\int_0^\infty \mathrm{d}z\,z^{-2}M_{q_1, q_1-n_1-\frac{1}{2}}(2\tau b_{11}^{\frac{1}{2}}z)\,M_{q_0, q_0-n_0-\frac{1}{2}}(2\tau b_{00}^{\frac{1}{2}}z). \end{aligned} \tag{2.2.6}$$

An explicit expression for this overlap integral in terms of the parameters q_m, a_{mm}, and b_{mm} is given in II.

PHILOSOPHICAL TRANSACTIONS OF THE ROYAL SOCIETY A MATHEMATICAL, PHYSICAL & ENGINEERING SCIENCES

The relative strengths of vibrational transitions are given by

$$I_{0,n_0\to 1,n_1} = |c_{n_0 n_1}|^2 \exp(-E_{0,n_0}/kT) \tag{2.2.7}$$

and the term values by

$$\frac{\Delta E}{hc} = \frac{1}{hc}[E_{1,n_1} - E_{0,n_0}], \tag{2.2.8}$$

where

$$E_{1,n_1} - E_{0,n_0} = (\epsilon_1 + \Delta\epsilon_1 - \epsilon_0 - \Delta\epsilon_0) - (D_2/r^2)\,((q_1 - n_1 - \tfrac{1}{2})^2 - (q_0 - n_0 - \tfrac{1}{2})^2). \tag{2.2.9}$$

This last equation suggests a grouping of the vibrational terms into sub-bands corresponding to $n_1 = n_0$, $n_1 = n_0 \pm 1$, etc. in exactly the same way as before. The only difference between this expression and that previously obtained lies in the definition of the parameters q_0 and q_1, which characterize the well depth and anharmonicity, and in the definition of the energies ϵ_0 and ϵ_1, which are now corrected for the effect of hydrogen bond formation on the ν(XH) force constant.

2.3. *The ν(XH) vibrational wavefunctions*

It is now necessary to find the eigenvalues ϵ_m and eigenfunctions $\chi_m(r)$ of (2.1.12) so that the parameters a_{mm} and b_{mm} of (2.1.18) and (2.1.19) can be evaluated. From (2.1.4) and (2.1.6) it follows that

$$V_1(r) + V_3(r, s_0) = (1 + c_1 + c_2)\,V_1(r). \tag{2.3.1}$$

It will be convenient to write

$$\tilde{D}_1 = D_1(1 + c_1 + c_2), \tag{2.3.2}$$

in terms of which equation (2.1.12) becomes

$$-\frac{\hbar^2}{2\mu_1}\frac{\mathrm{d}^2\chi_m(r)}{\mathrm{d}r^2} + \tilde{D}_1(1 - \mathrm{e}^{-\beta(r-r_0)})^2\chi_m(r) = \epsilon_m\chi_m(r). \tag{2.3.3}$$

In other words, the potential governing the ν(XH) vibration of the hydrogen-bonded species near its equilibrium X..Y separation is being taken as a Morse function which has the same exponent as the Morse function appropriate for the free XH molecule, but which has its dissociation energy parameter, and hence – more importantly – its second derivative at the minimum, reduced in the ratio $(1 + c_1 + c_2)$. The eigenfunctions of (2.3.3) may be found by a trivial modification of the analysis of II, and are given by

$$\chi_m(r) = \zeta^{-\frac{1}{2}}N_m M_{\tilde{k},\tilde{k}-m-\frac{1}{2}}(\zeta), \tag{2.3.4}$$

where

$$\tilde{k} = (2\mu_1\tilde{D}_1)^{\frac{1}{2}}/\beta\hbar, \tag{2.3.5}$$

$$\zeta = 2\tilde{k}\exp(-\beta(r - r_0)), \tag{2.3.6}$$

and $M_{\tilde{k},\tilde{k}-m-\frac{1}{2}}(\zeta)$ is a confluent hypergeometric function (Whittaker & Watson 1927). The corresponding energy eigenvalues are

$$\epsilon_m = (m + \tfrac{1}{2})\,(2\tilde{k} - m - \tfrac{1}{2})\,\tilde{D}_1/\tilde{k}^2. \tag{2.3.7}$$

The evaluation of the level shifts $\Delta\epsilon_m$ of (2.1.15) and the parameters a_{mm} and b_{mm} of (2.1.18) and (2.1.19) is outlined in appendix A. The results are

$$\Delta\epsilon_0 = -(c_1 + c_2)\,D_1/2\tilde{k}, \tag{2.3.8}$$

$$\Delta\epsilon_1 = -3(c_1 + c_2)\,D_1/2\tilde{k}, \tag{2.3.9}$$

$$a_{00} = (2\tilde{k})^\eta\Gamma(2\tilde{k} - 1 - \eta)/\Gamma(2\tilde{k} - 1) - c_1 D_1/4\tilde{k}D_2, \tag{2.3.10}$$

$$b_{00} = (2\tilde{k})^{2\eta}\Gamma(2\tilde{k}-1-2\eta)/\Gamma(2\tilde{k}-1) + c_2 D_1/2\tilde{k}D_2, \tag{2.3.11}$$

$$a_{11} = (2\tilde{k})^{\eta}\left(1+\frac{\eta+\eta^2}{2\tilde{k}-2}\right)\Gamma(2\tilde{k}-3-\eta)/\Gamma(2\tilde{k}-3) - 3c_1 D_1/4\tilde{k}D_2 \tag{2.3.12}$$

and

$$b_{11} = (2\tilde{k})^{2\eta}\left(1+\frac{2\eta+4\eta^2}{2\tilde{k}-2}\right)\Gamma(2\tilde{k}-3-2\eta)/\Gamma(2\tilde{k}-3) + 3c_2 D_1/2\tilde{k}D_2, \tag{2.3.13}$$

where

$$\eta = \alpha\gamma/\beta. \tag{2.3.14}$$

3. Reconstruction of the spectrum

3.1. *Deducing the nature of the potential energy surface of* $Me_2O.HCl$

In order to apply these results it is necessary to specify the three atomic masses m_X, m_H and m_Y, the Morse function parameters D_1 and β characterizing $V_1(r)$ and D_2 and α characterizing $V_2(R)$, and the additional parameters c_1 and c_2 introduced in $V_3(r,s)$. D_1 and β are easily found in terms of the ν(XH) stretching frequency and the anharmonicity constant of the free XH molecule; details are given in II. D_2 is known from experiment in certain cases, including those of the $Me_2O.HCl$ (Seel 1966) and $Me_2O.HF$ species (Thomas 1971*a*). The determination of α, c_1 and c_2 is rather more complicated.

In the case of $Me_2O.HCl$ and certain other similar species two further spectroscopic data are available: the frequency of the central peak of the spectrum and the frequency of the hydrogen bond vibration. From (2.2.5) it follows that in the ground state of the ν(XH) vibration the ν(HX..Y) vibrational levels are given by

$$E_{0,n} = (n+\tfrac{1}{2})(2D_2 q_0/\tau^2) - (n+\tfrac{1}{2})^2(D_2/\tau^2) + \text{const.}; \tag{3.1.1}$$

ignoring the anharmonicity correction one can identify the vibrational frequency with $2D_2 q_0/\tau^2$. From (2.2.2) and (2.2.3) this is equal to $\alpha\hbar(2D_2/\mu_2)^{\frac{1}{2}}(a_{00}/b_{00}^{\frac{1}{2}})$. The ratio $a_{00}/b_{00}^{\frac{1}{2}}$ depends in a complicated way on all the energy surface parameters, but is necessarily of the order of unity. Knowledge of the ν(XH..Y) frequency thus enables a rough estimate of α to be obtained.

From (2.2.9) and (2.3.7) the term value of a particular $|0, n_0\rangle \rightarrow |1, n_1\rangle$ transition is related to $\epsilon_1 - \epsilon_0$, and hence to $(1+c_1+c_2)^{\frac{1}{2}}$; however, the correction terms in (2.2.9) depend on the a_{mm} and b_{mm}, which involve all six energy surface parameters. The experimental data thus impose two constraints on the three unknown parameters, so that only one quantity is indeterminate. If c_1 is specified, the values of c_2 and α can in principle be deduced by solving the pair of non-linear simultaneous equations

$$E_{1,n_1} - E_{0,n_0} = (\epsilon_1 + \Delta\epsilon_1 - \epsilon_0 - \Delta\epsilon_0) - (D_2/\tau^2)\left((q_1 - n_1 - \tfrac{1}{2})^2 - (q_0 - n_0 - \tfrac{1}{2})^2\right) \tag{3.1.2}$$

and

$$E_{0,n+1} - E_{0,n} = 2D_2(q_0 - n - 1)/\tau^2. \tag{3.1.3}$$

Since prior estimates of α and c_2 are available there is no difficulty about solving these equations iteratively: a method due to Powell (1968) has proved very satisfactory in practice. Thus it is possible to explore various forms of the potential energy surface by specifying c_1, finding the values of c_2 and α which satisfy the constraints imposed by the experimental data, and obtaining the values of the a_{mm} and b_{mm} which characterize the effective potential curves $U_{00}(s)$ and $U_{11}(s)$ for the ν(XH..Y) vibration. The term values and intensities of all $|0, n_0\rangle \rightarrow |1, n_1\rangle$ transitions can then be calculated from (2.2.7) and (2.2.9) in much the same way as in II.

In order to study the temperature dependence of the reconstructed spectrum it is convenient to group all transitions into sub-bands according to the value of $n_1 - n_0 = \Delta n$, and to sum the intensities of all transitions within each sub-band. The ratios of these calculated sub-band intensities can then be studied as a function of temperature for any particular choice of the parameter c_1.

Results for the $Me_2O.HCl$ system are presented graphically in figure 1. The input parameters used are $m_X = 35.5u$, $m_H = 1.0u$, $m_Y = 46.1u$, $D_1 = 42950\ cm^{-1}$, $\beta = 1.738 \times 10^8\ cm^{-1}$, and $D_2 = 2750\ cm^{-1}$. The values of D_1 and β are chosen to reproduce the known frequency and anharmonicity constant $E_1 = 2989\ cm^{-1}$ and $xE_1 = 52.1\ cm^{-1}$ of free HCl (Herzberg 1950); D_2 is based on the work of Seel (1966). The term value of the $|0, 0\rangle \rightarrow |1, 1\rangle$ transition is taken as $2570\ cm^{-1}$, in accordance with the assignment of Lassègues & Huong (1972) and Bertie & Falk (1973), and that of the $|0, 0\rangle \rightarrow |0, 1\rangle$ transition is taken as $100\ cm^{-1}$, a value deduced from the spacing of the

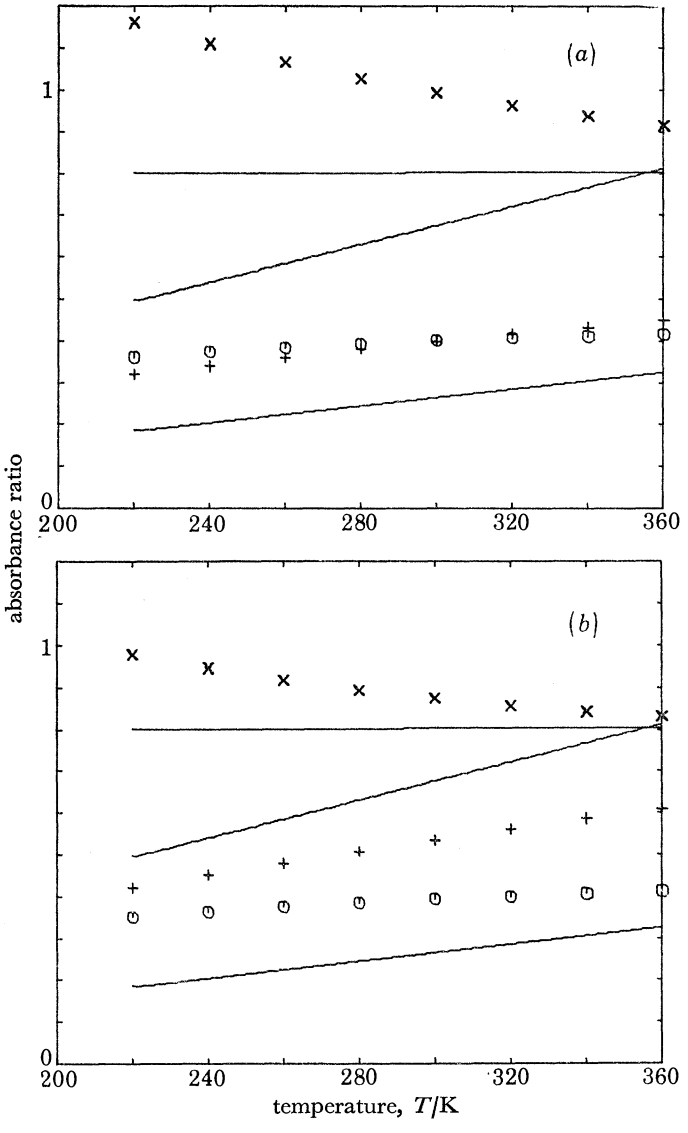

FIGURE 1. For description see opposite.

incompletely resolved structure in the spectrum.† The calculated intensities of the sub-bands $\Delta n = 1, -0$, and 2 responsible for the structure observed at 2360, 2470 and 2660 cm^{-1}, relative to the intensity of the main $\Delta n = 1$ sub-band centred at 2570 cm^{-1}, are plotted as a function of temperature between 220 and 360 K for values of c_1 between 0.05 and 0.20. The experimental intensity ratios of Lassègues & Huong (1972) are given for comparison in each case. It appears

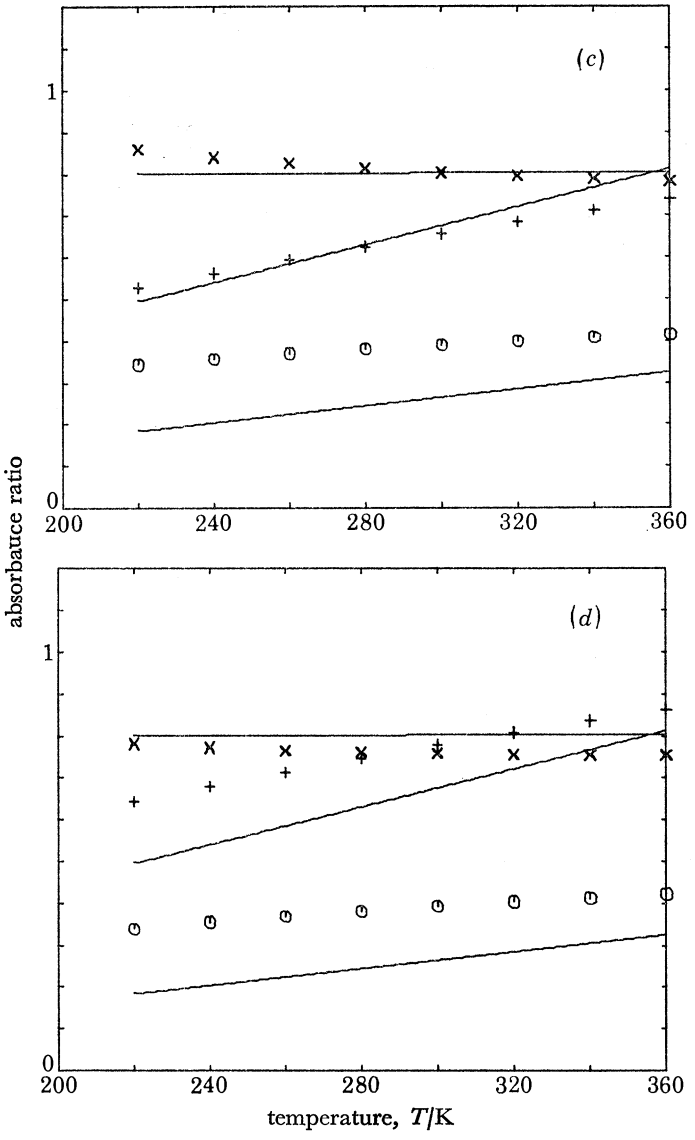

FIGURE 1. Comparison of observed and calculated absorbance ratios A_v/A_{2570} as a function of temperature for different values of the coupling parameter c_1. Calculated values of the ratios A_{2660}/A_{2570}, A_{2470}/A_{2570} and A_{2360}/A_{2470} are denoted by +, ×, and ⊙ respectively. The best straight lines fitted through the experimental data points of Lassègues & Huong are given for comparison in each case. In figure 1*a*, $c_1 = 0.05$, $c_2 = -0.302$; in figure 1*b*, $c_1 = 0.10$, $c_2 = -0.342$; in figure 1*c*, $c_1 = 0.15$, $c_2 = -0.382$; and in figure 1*d*, $c_1 = 0.20$, $c_2 = -0.420$.

† This is the value originally suggested by Bertie & Millen (1965). The values obtained by far infrared spectroscopy are in the region of 120 cm^{-1} (Belozerskaya & Shchepkin 1966; Lassègues & Huong 1972; Bertie & Falk 1973). The position of the maximum of a broad band in the far infrared does not give a reliable indication of the vibration frequency unless a correction is made for various frequency-dependent factors in the theoretical intensity expression, and it is possible that this is the origin of the discrepancy.

that reasonably satisfactory agreement is obtained with c_1 equal to 0.15, to which values of -0.38 for c_2 and 1.03×10^8 cm^{-1} for α are found to correspond.

It has not been found possible to obtain even a qualitatively correct account of the temperature dependence of the intensity ratios on the basis of the original assignment of Bertie & Millen (1965), which identified the peak at 2570 cm^{-1} with the $|0, 0\rangle \rightarrow |1, 0\rangle$ transition. The present results thus strongly support the new assignment of Lassègues & Huong (1972) and Bertie & Falk (1973), and confirm the theoretical calculations of E. Maréchal & Bouteiller (1974), which were based on a somewhat simpler model.

It is difficult to judge how accurately these three parameters are determined; however, the errors to which c_1 and c_2 are subject can hardly be less than 20 %. Although the calculated Morse exponent α is not particularly sensitive to the choice of c_1, it does depend directly on the experimental value of the ν(XH..Y) frequency, about which there is some ambiguity owing to the discrepancies between the values derived from near and far infrared experimental work; and it

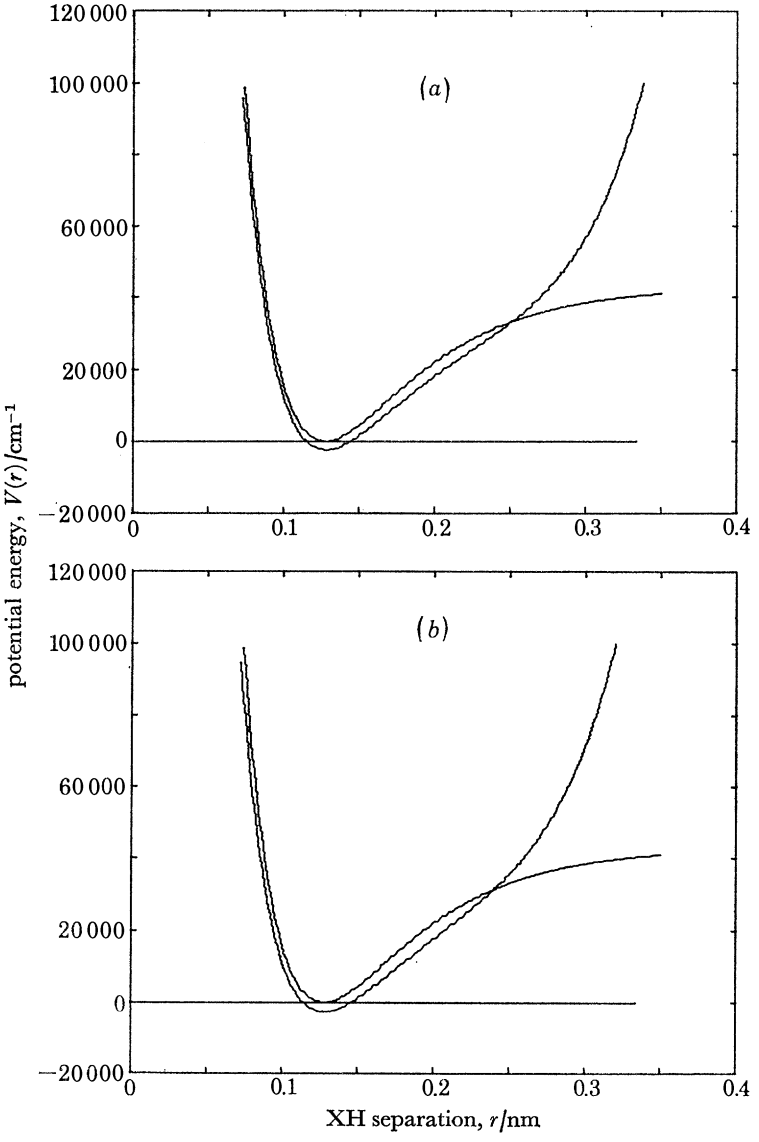

FIGURE 2. For description see opposite.

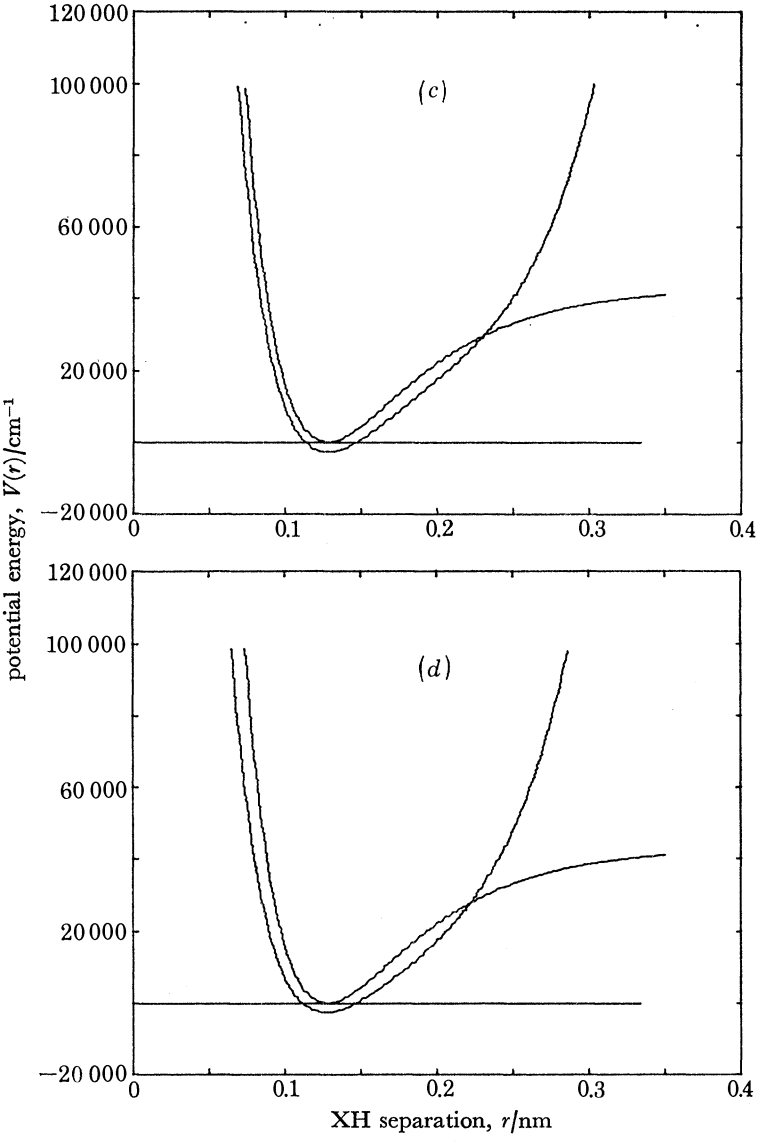

FIGURE 2. The effect of varying hydrogen bond length X..Y on the potential for the ν(XH) motion. In figure 2*a*, X..Y = 0.35 nm; in figure 2*b*, X..Y = 0.33 nm; in figure 2*c*, X..Y = 0.31 nm, the equilibrium value; and in figure 2*d*, X..Y = 0.29 nm. The Morse function which best represents the interatomic potential of free HCl is given in each case for comparison.

also depends directly on D_2, which is not very accurately known. Furthermore, the tacit assumption that the peak absorbance ratios measured by Lassègues & Huong can be identified with the integrated intensity ratios of resolved vibrational sub-bands is open to serious objection, and leads to further uncertainties.

Despite these reservations about the accuracy of the numerical parameters obtained, it seems reasonable to believe that the potential energy surface for $Me_2O.HCl$ is fairly well represented by a function of form (2.1.3) with the following parameters:

$$D_1 = 42950\,\mathrm{cm}^{-1}, \quad \beta = 1.738 \times 10^8\,\mathrm{cm}^{-1}, \quad D_2 = 2750\,\mathrm{cm}^{-1},$$
$$\alpha = 1.03 \times 10^8\,\mathrm{cm}^{-1}, \quad c_1 = 0.15, \quad \text{and} \quad c_2 = -0.38.$$

The remainder of the paper explores the consequences of this in detail.

It should be noted, however, that this representation of the potential energy surface cannot be accurate when the separation between the X and Y atoms is small. In particular, for any fixed value of s the function $V_1(r) + V_3(r, s)$ will not have a minimum at $r = r_0$ unless

$$1 + c_1 e^{-\alpha(s-s_0)} + c_2 e^{-2\alpha(s-s_0)} > 0.$$

If c_2 is negative, this condition will be violated for small s, and with the above parameter values it follows that the model potential energy surface has quite the wrong geometrical properties unless $s - s_0$ exceeds -0.06 nm. Only relatively highly excited states of the ν(XH..Y) motion, with $v = 15$ or more, have such large vibrational amplitudes, however, and the deficiencies of the representation ought not to have too pronounced an effect on calculations involving low-lying excited states.

The form of the potential function $V(r, s)$ of (2.1.3) for various fixed values of the X..Y separation is illustrated in figure 2, which is drawn accurately to scale. As the X..Y distance is reduced, the curvature of the function at the minimum decreases, though the function also becomes more steeply repulsive as r increases owing to the effect of $V_2(R)$. The curves become progressively less accurate as the X..Y separation is reduced below its equilibrium value $r_0 + R_0$, and eventually the representation breaks down completely as the curvature at the minimum approaches zero. The form of $V(r, s)$ is not accurate enough to reflect the well-known increase in the equilibrium X–H separation which accompanies hydrogen bond formation (Sheppard 1959).

3.2. *The effective potential curves* $U_{00}(s)$ *and* $U_{11}(s)$

Thus far the argument has been concerned entirely with the total intensities of vibrational sub-bands. Owing to the differences in the anharmonicities of the potential curves $U_{00}(s)$ and $U_{11}(s)$ the various transitions in each of these sub-bands will not coincide, and the question arises whether this is sufficient to explain the formation of a continuous broad spectrum with a peak and shoulder structure.

Detailed results for the Me_2O.HCl system at 300 K are presented in table 1. These have been normalized so that the intensity of the strongest sub-band at 2570 cm^{-1} is unity. It is seen that the positions of the centres of the component sub-bands are well separated, owing to the rather close spacing of terms within each.

It is instructive to compare these results with those of table 1 of II, in which only the kinematic coupling mechanism was considered. The Franck–Condon factors for $|0, n\rangle \rightarrow |1, n \pm 1\rangle$ transitions are now much larger, which is indicative of an increase in the separation $|s_{11} - s_{00}|$ between the minima of $U_{00}(s)$ and $U_{11}(s)$; and the term value of the $|0, 0\rangle \rightarrow |1, 0\rangle$ transition is now 2462 cm^{-1}, as opposed to 2930 cm^{-1} in II and to 2885 cm^{-1} for the $v = 0$ to $v = 1$ transition in free HCl, which shows that the effective potential $U_{11}(s)$ is now appreciably deeper than $U_{00}(s)$ instead of being slightly shallower.

The parameters which characterize the effective potentials for Me_2O.HCl are given in table 2; those of II are also presented for comparison. The most striking feature concerns the positions of the minima of $U_{mm}(s)$. The kinematic coupling effect treated in II tends to displace both minima towards greater values of the coordinate, this being more pronounced for the upper curve than for the lower. When allowance is made in addition for the electronic coupling effect the minima are both displaced towards smaller values of the coordinate. The electronic coupling thus acts in the opposite sense to the kinematic coupling effect and completely outweighs it, both as regards the depth of the wells and the positions of the minima. Making proper allowance for

TABLE 1. CALCULATED VIBRATIONAL TERM VALUES AND INTENSITIES FOR $Me_2O.HCl$ AT 300 K

transition	term value / cm^{-1}	Franck–Condon factor	intensity	sub-band intensity
$\|0,1\rangle \rightarrow \|1,0\rangle$	2362.3	0.297	0.230	
$\|0,2\rangle \rightarrow \|1,1\rangle$	2371.7	0.236	0.114	
$\|0,3\rangle \rightarrow \|1,2\rangle$	2381.0	0.111	0.034	
$\|0,4\rangle \rightarrow \|1,3\rangle$	2390.3	0.027	0.005	
$\|0,5\rangle \rightarrow \|1,4\rangle$	2399.6	0.000	0.000	0.39
$\|0,6\rangle \rightarrow \|1,5\rangle$	2408.9	0.013	0.001	
$\|0,7\rangle \rightarrow \|1,6\rangle$	2418.2	0.043	0.002	
$\|0,8\rangle \rightarrow \|1,7\rangle$	2427.5	0.071	0.002	
$\|0,9\rangle \rightarrow \|1,8\rangle$	2436.8	0.076	0.002	
$\|0,0\rangle \rightarrow \|1,0\rangle$	2462.4	0.534	0.665	
$\|0,1\rangle \rightarrow \|1,1\rangle$	2469.9	0.076	0.059	
$\|0,2\rangle \rightarrow \|1,2\rangle$	2477.5	0.001	0.001	
$\|0,3\rangle \rightarrow \|1,3\rangle$	2485.0	0.053	0.016	
$\|0,4\rangle \rightarrow \|1,4\rangle$	2492.6	0.116	0.023	0.80
$\|0,5\rangle \rightarrow \|1,5\rangle$	2500.1	0.149	0.019	
$\|0,6\rangle \rightarrow \|1,6\rangle$	2507.7	0.147	0.012	
$\|0,7\rangle \rightarrow \|1,7\rangle$	2515.2	0.120	0.006	
$\|0,8\rangle \rightarrow \|1,8\rangle$	2522.8	0.084	0.003	
$\|0,0\rangle \rightarrow \|1,1\rangle$	2569.9	0.370	0.461	
$\|0,1\rangle \rightarrow \|1,2\rangle$	2575.7	0.405	0.314	
$\|0,2\rangle \rightarrow \|1,3\rangle$	2581.5	0.308	0.154	
$\|0,3\rangle \rightarrow \|1,4\rangle$	2587.3	0.185	0.060	
$\|0,4\rangle \rightarrow \|1,5\rangle$	2593.1	0.085	0.018	1.00
$\|0,5\rangle \rightarrow \|1,6\rangle$	2598.8	0.024	0.003	
$\|0,6\rangle \rightarrow \|1,7\rangle$	2604.6	0.001	0.000	
$\|0,7\rangle \rightarrow \|1,8\rangle$	2610.4	0.006	0.000	
$\|0,8\rangle \rightarrow \|1,9\rangle$	2616.2	0.040	0.002	
$\|0,0\rangle \rightarrow \|1,2\rangle$	2675.7	0.087	0.108	
$\|0,1\rangle \rightarrow \|1,3\rangle$	2679.7	0.192	0.149	
$\|0,2\rangle \rightarrow \|1,4\rangle$	2683.8	0.280	0.135	
$\|0,3\rangle \rightarrow \|1,5\rangle$	2687.8	0.336	0.102	
$\|0,4\rangle \rightarrow \|1,6\rangle$	2691.8	0.358	0.069	0.65
$\|0,5\rangle \rightarrow \|1,7\rangle$	2695.8	0.350	0.043	
$\|0,6\rangle \rightarrow \|1,8\rangle$	2699.9	0.319	0.026	
$\|0,7\rangle \rightarrow \|1,9\rangle$	2703.9	0.270	0.014	
$\|0,8\rangle \rightarrow \|1,10\rangle$	2707.9	0.007	0.000	

TABLE 2. THE PARAMETERS CHARACTERIZING THE EFFECTIVE POTENTIALS FOR $Me_2O.HCl$

parameter	both coupling mechanisms included	kinematic coupling alone
τ	55.9	55.9
a_{00}	0.998	1.019
b_{00}	0.932	1.044
a_{11}	0.996	1.058
b_{11}	0.805	1.138
q_0	57.8	55.7
q_1	62.0	55.4
$(s_{00}-s_0)$/pm	−6.6	+2.3
$(s_{11}-s_0)$/pm	−20.6	+7.1
D_{00}/cm^{-1}	2940	2730
D_{11}/cm^{-1}	3383	2701

the electronic coupling effect thus leads to a description where the hydrogen bond is stronger and shorter in the first ν(XH) excited state than in the ground state,† in complete agreement with the intuitive argument of Sheppard (1959). This is illustrated in figure 3.

The predicted shortening of the hydrogen bond is very pronounced, and this has two major consequences. First, the question of vibrational predissociation treated in I needs re-examination, since the potential curves $U_{00}(s)$ and $U_{11}(s)$ are now found to intersect. This is discussed in § 5 below. Secondly, the moment of inertia of the complex is appreciably smaller in the upper ν(XH) state than in the lower, and this affects the rotational structure associated with each $|0, n_0\rangle \rightarrow |1, n_1\rangle$ transition.

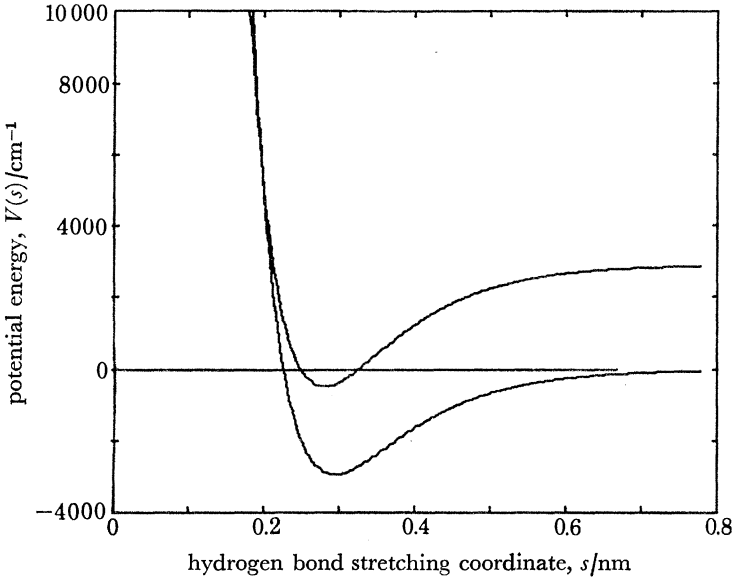

FIGURE 3. The predicted effective potentials $U_{00}(s)$ and $U_{11}(s)$ for the ν(XH..Y) motion. It should be noted that the upper curve is deeper than the lower and has its minimum at a smaller value of the coordinate, and that the two curves intersect.

3.3 *The vibration–rotation interaction*

In order to explore qualitatively the effect of vibration–rotation coupling on the spectrum it is convenient to retain the simplifying assumption of a linear triatomic complex. The total angular momentum J of the complex is a constant of the motion, and the energies of $|m, n, J\rangle$ states can be evaluated by adding a centrifugal potential $V_J(r, s)$ to the vibrational hamiltonian,‡ where

$$V_J(r, s) = J(J+1)\,\hbar^2/2I(r, s) \tag{3.3.1}$$

and

$$I(r, s) = \mu_1 r^2 + \mu_2 s^2. \tag{3.3.2}$$

The centrifugal potential will be treated as a perturbation. The first order correction to the energy is given by

$$W^{(1)}_{m,n,J} = \langle m, n|V_J(r, s)\,|m, n\rangle, \tag{3.3.3}$$

† A similar result has previously been obtained by E. Maréchal & Bouteiller (1974).

‡ This simplified treatment of the rotation of a polyatomic molecule neglects any contribution to the vibration–rotation interaction which may arise from Coriolis forces. Such interactions are not likely to be very significant in the present context, since the ν(XH) frequency is much greater than those of the other vibrational modes considered. The treatment is perhaps more nearly described as that for a pseudo-diatomic molecule.

and the second order correction by

$$W^{(2)}_{m,n,J} = \sum_{m',n' \neq m,n} \frac{|\langle m,n|\, V_J(r,s)\, |m',n'\rangle|^2}{E_{m,n} - E_{m',n'}}. \tag{3.3.4}$$

$W^{(2)}_{m,n,J}$ may in principle be evaluated by expanding the centrifugal potential in Taylor series about the centre of motion (r_0, s_{mm}), but there is little point in retaining any terms beyond the first, as they only provide a small correction to the moment of inertia resulting mainly from vibrational anharmonicity. To a good approximation,

$$W^{(1)}_{m,n,J} = J(J+1)\,\hbar^2/2I(r_0, s_{mm}), \tag{3.3.5}$$

which is independent of the ν(XH..Y) quantum number n, but depends on the ν(XH) quantum number m because of its striking effect on the hydrogen bond length. To this order of approximation the hydrogen bond length is treated as independent of $J(J+1)$, since the zero order hamiltonian describes a molecule which is fixed in space.

Corrected to first order in $V_J(r,s)$, the vibrational wavefunctions will depend on $J(J+1)$, as will the expectation value of the X..Y separation. The second order energy correction $W^{(2)}_{m,n,J}$, proportional to $J^2(J+1)^2$, can thus be identified as a correction for centrifugal distortion; its dependence on m is a consequence of the variation of the hydrogen bond length with the ν(XH) vibrational state, and its dependence on n is largely a consequence of the ν(XH..Y) anharmonicity.

Thomas & Thompson (1970) have identified P branch band heads in the spectrum of $CH_3CN.HCl$ and have explained their formation in terms of differences in the rotational constants for the $v = 0$ and $v = 1$ states of the ν(XH) vibration. Lascombe, Lassègues & Huong (1973) have suggested that centrifugal distortion contributes to the broadening of the spectra of hydrogen-bonded species, and have discussed this in terms of a classical model. Both these mechanisms may be expected to influence the spectrum and it is of considerable interest to determine which of them is more important. A simple way of resolving the issue is to calculate the first order and second order corrections separately.

The rotational constants B_0 and B_1 of the linear complex in its ground and first excited ν(XH) states are defined in terms of (3.3.5) as

$$B_m = h/8\pi^2 cI(r_0, s_{mm}). \tag{3.3.6}$$

Provided that r_0 and s_0 are known, these are easily found from the results of table 2. Little error will be introduced by taking $r_0 = 0.127$ nm, which is the value for free HCl (Herzberg 1950). However, s_0 is not known from experiment, and it is necessary to assume a value for it: $s_0 = 0.31$ nm, as suggested by Bertie & Falk (1973), seems not unreasonable.

With this choice the rotational contents are found to be $B_0 = 0.088(5)$ cm^{-1} and $B_1 = 0.097(2)$ cm^{-1}. The wavenumbers of vibration–rotation lines in the P and R branches arising from $|0, n_0, J\rangle \rightarrow |1, n_1, J \pm 1\rangle$ transitions will be

$$\nu_R = (E_{1,n_1} - E_{0,n_0})/hc + 2B_1 + (3B_1 - B_0)\,J + (B_1 - B_0)\,J^2 \tag{3.3.7a}$$

and

$$\nu_P = (E_{1,n_1} - E_{0,n_0})/hc - (B_1 + B_0)\,J + (B_1 - B_0)\,J^2. \tag{3.3.7b}$$

Since B_1 is greater than B_0, ν_P will decrease initially until it reaches its minimum value

$$\nu_{P\min} = (E_{1,n_1} - E_{0,n_0})/hc - \tfrac{1}{4}(B_1 + B_0)^2/(B_1 - B_0), \tag{3.3.8}$$

when

$$J_{\min} = \tfrac{1}{2}(B_1 + B_0)/(B_1 - B_0), \tag{3.3.9}$$

and thereafter it will increase with J. Lines of the P branch for which J exceeds $2J_{\min}$ will be interspersed among lines of the R branch, and if $J_{\min}$ is sufficiently small this will lead to a highly asymmetric band. In the present case $J_{\min} = 11$, and the P branch terms are positive for $J \geqslant 22$. The most highly populated state at room temperature corresponds to $J = 34$.

The vibration–rotation band contour deduced for $Me_2O.HCl$ at 300 K is shown in figure 4. It has been constructed by calculating the wavenumbers and Hönl–London factors of all $J \rightarrow J \pm 1$ transitions up to $J = 100$, sorting the lines into ascending order of frequency, grouping them, introducing a triangular instrumental width of 2 cm^{-1}, and evaluating the intensity at 1 cm^{-1} intervals. Owing to the large difference between B_1 and B_0 the P branch band head is extremely pronounced; indeed, $\nu_{P_{\min}}$ is only 1 cm^{-1} less than the vibrational term difference. However, the intensity associated with the band head is only a fraction of that for the entire P branch, much of which is merged with the R branch. Since the coefficient of J^2 in (3.3.6) is fairly large, the spacing between lines in the R branch increases rapidly with J, and this results in a long, sloping profile extending over nearly 100 cm^{-1}.

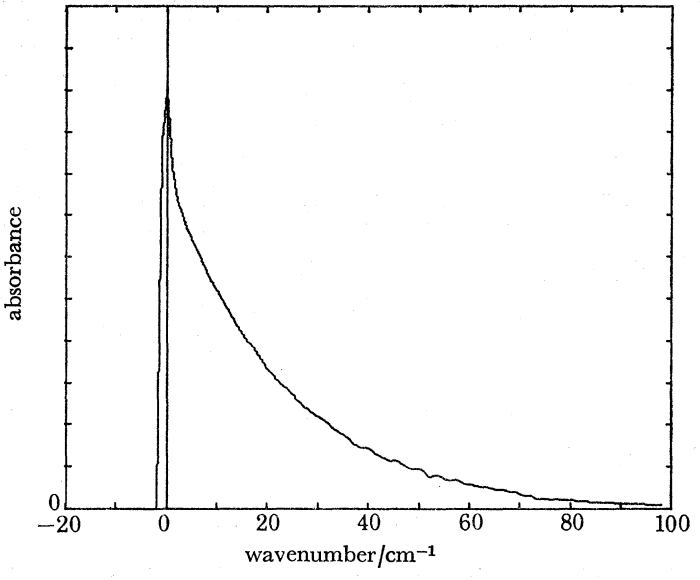

FIGURE 4. The calculated rotational structure associated with each $|0, n_0\rangle \rightarrow |1, n_1\rangle$ transition. A linear triatomic model of $Me_2O.HCl$ is assumed and centrifugal distortion is neglected. An instrumental width of 2 cm^{-1} has been introduced artificially.

In order to evaluate the second order correction it is simplest to ignore the dependence of $V_J(r, s)$ on r, which is a good approximation since μ_1 is considerably smaller than μ_2, and also to ignore the anharmonicity of the ν(XH..Y) motion. With these simplifications, the summation in (3.3.4) reduces to

$$W^{(2)}_{m,n,J} = \sum_{n' \neq n} \frac{|\langle m, n| V_J(r_0, s) |m, n'\rangle|^2}{E_{m,n} - E_{m,n'}}. \tag{3.3.10}$$

$V_J(r_0, s)$ is now expanded in Taylor series about s_{mm}, with only the term linear in s being retained, and the ν(XH..Y) wavefunctions are regarded as harmonic oscillator eigenstates with energies $(n + \frac{1}{2})\hbar\omega_m$, where

$$\hbar\omega_m = 2D_2 q_m / r^2 \tag{3.3.11}$$

by appeal to (3.1.1). All terms in the summation vanish except those for which $n' = n \pm 1$, and (3.3.10) becomes

$$W^{(2)}_{m,n,J}\left(\frac{1}{\hbar\omega_m}\right)\left[\frac{\partial V_J(r_0,s)}{\partial s}\right]^2_{s_{mm}}[\langle n|(s-s_{mm})|n-1\rangle^2-\langle n|(s-s_{mm})|n+1\rangle^2]. \quad (3.3.12)$$

The quantity in parentheses is easily found to be $-(\hbar/2\mu_2\omega_m)$ so that to a good approximation

$$W^{(2)}_{m,n,J} = -\left(\frac{1}{2\mu_2\omega_m^2}\right)\left\{\frac{J(J+1)\hbar^2}{2I^2(r_0,s_{mm})}\left[\frac{\partial I(r_0,s)}{\partial s}\right]_{s_{mm}}\right\}^2. \quad (3.3.13)$$

The rotational terms in the ν(XH) state designated by m can thus be written

$$F_m(J) = B_m[1-u_m J(J+1)]\,J(J+1), \quad (3.3.14)$$

the definition of u_m in terms of (3.3.13) and (3.3.6) being straightforward. It is found that $u_0 = 0.31\times10^{-5}$ and $u_1 = 0.37\times10^{-5}$. Evidently the centrifugal distortion correction is only significant for large values of J, in excess of perhaps 100. The effect of including the correction is shown in figure 5. Comparison with figure 4 shows that only the extreme wing of the R branch is affected.

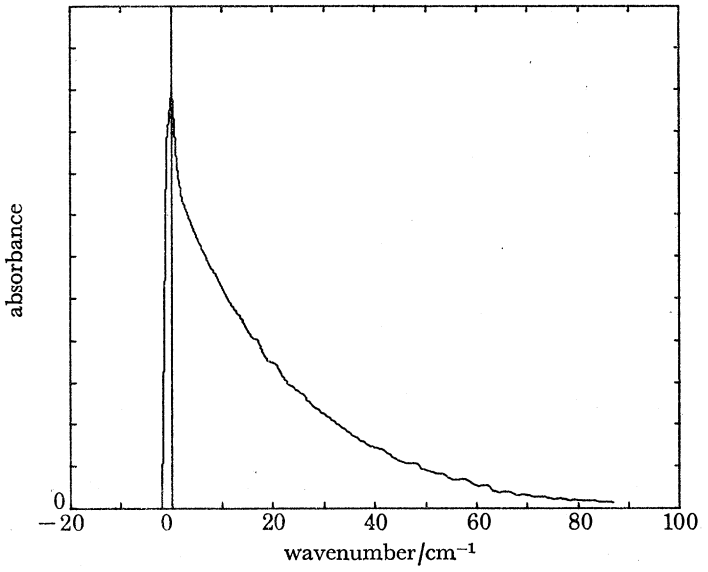

FIGURE 5. The calculated rotational structure in $Me_2O.HCl$, assuming a linear triatomic model and including the effects of centrifugal distortion.

It is safe to conclude, therefore, that the mechanism discussed by Thomas & Thompson (1970) in connection with $CH_3CN.HCl$ is of central importance in determining the profile of the $Me_2O.HCl$ spectrum; the origin of the effect is the anharmonic coupling between the ν(XH) and ν(XH..Y) modes, which leads to a marked shortening of the complex in the first ν(XH) excited state. The suggestion of Lascombe, Lassègues & Huong, that centrifugal distortion will be abnormally large in hydrogen-bonded species and may influence the infrared spectrum is perfectly correct, but the effect is nevertheless only of secondary importance. In absolute terms it is quite large; but in comparison with the spectacular first order effect it is insignificant. Experimental evidence has been adduced by Bertie & Falk (1973) to show that centrifugal distortion cannot greatly affect the ν(XH) ground state, and this is entirely consistent with the present argument. The calculation of Bouteiller & E. Maréchal (1975) also shows clearly the importance

of vibration–rotation coupling in $Me_2O.HCl$, but it obtains the rotational energy only to first order in $J(J+1)$ and does not treat centrifugal distortion.

Strictly speaking, the $Me_2O.HCl$ complex should not be treated as a linear molecule: it is rather more satisfactory to regard it as a symmetric top.† The moment of inertia about the molecular axis is expected to be approximately one-tenth of that about a perpendicular through the centre of mass, and it will not depend much on the state of the ν(XH) vibration. By taking into account all transitions for which $\Delta J = \pm 1$ or 0 and $\Delta K = 0$ the rotational profile of figure 6 is obtained.‡ It does not differ greatly from that of figure 5, though there is less fine structure owing to the much greater number of rotational transitions involved.

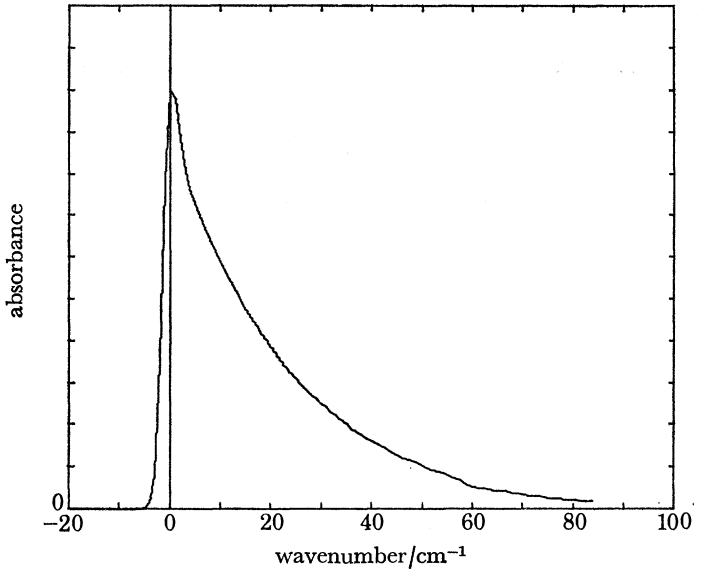

FIGURE 6. The calculated rotational structure in $Me_2O.HCl$, assuming the complex to be a symmetric top.

The question now arises whether the spectrum of $Me_2O.HCl$ can be understood in terms of ν(XH) $\pm n\nu$(XH..Y) Franck–Condon transitions and vibration–rotation interaction alone. A theoretical spectrum, for a linear complex, is shown in figure 7; this has been constructed by calculating the frequencies and intensities of all $|0, n_0, J\rangle \rightarrow |1, n_1, J \pm 1\rangle$ transitions for values of n_0 up to 8 and values of J up to 100, and then sorting and grouping the lines and introducing an instrumental width as before. A very similar spectrum, though somewhat smoother in contour, is obtained by treating the complex as a symmetric top.

The reconstructed spectrum is not in satisfactory agreement with experiment; the major difficulties are that the vibrational sub-bands do not merge to form a continuous band, and that

† In practice all three principal moments of inertia of the complex will differ, but since the two larger principal moments will be of similar magnitude a symmetric top approximation is not unreasonable.

‡ The neglect of transitions for which $\Delta K = \pm 1$ tacitly assumes that the Cl–H...0 direction is a symmetry axis of the complex, i.e. that the configuration about the oxygen atom is planar and that the ν(XH) band is a parallel band. In practice it seems likely that the configuration will be pyramidal, in which case the ν(XH) band will be hybrid in character, with a series of perpendicular sub-bands overlapping the parallel band. A rough calculation suggests that the perpendicular component band will be broader than the parallel band but appreciably weaker, and thus of lesser importance. Nevertheless, it is possible that the present calculation, by neglecting the perpendicular component, underestimates the overall breadth of the rotational structure in the ν(XH) band and exaggerates the relative importance of the band heads in the parallel component.

the reconstructed spectrum has a rather jagged appearance as a result of the band heads associated with the constituent Franck–Condon transitions. In the circumstances it seems likely that combinations involving low-frequency bending modes of the hydrogen bond contribute to the spectrum. The importance of these has been stressed by Thomas & Thompson (1970), Thomas (1971*b*) and Bertie & Falk (1973) in connection with the spectra of $CH_3CN.HCl$, $CH_3CN.HF$ and $Me_2O.HCl$ respectively.

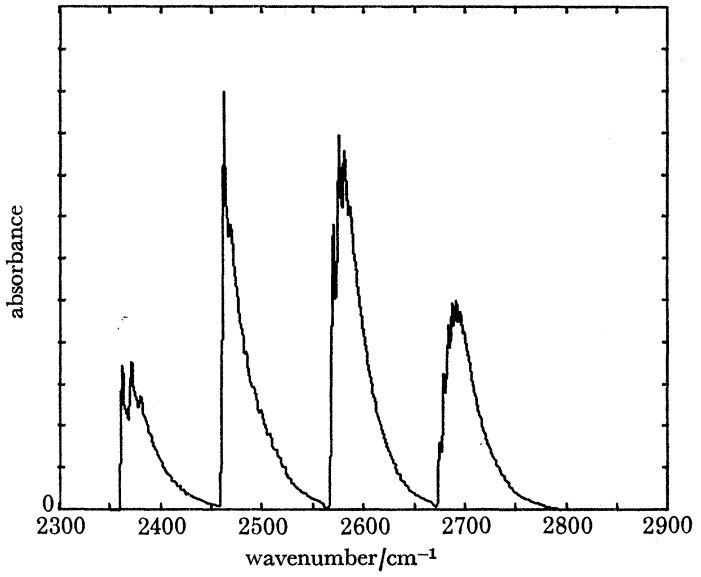

FIGURE 7. The calculated profile of the ν(XH) absorption band in $Me_2O.HCl$.

4. THE EFFECT OF DEUTERIUM SUBSTITUTION

4.1. *The effect on the potentials* $U_{00}(s)$ *and* $U_{11}(s)$

The potential curves $U_{00}(s)$ and $U_{11}(s)$ are determined by the parameters a_{mm} and b_{mm} of (2.1.18) and (2.1.19), and in order to understand the effect of isotopic substitution it is necessary to examine the dependence of these parameters on the atomic masses. To a good approximation the parameters α, β, c_1, c_2, D_1, and D_2 used to characterize the potential energy surface should be unaffected by deuterium substitution; the reduced mass μ_1 will be nearly doubled, however, and μ_2 and γ will change by a small amount. The main effect will be to increase the parameter $\tilde{k}$ of (2.3.5) by a factor of nearly $2^{\frac{1}{2}}$, so that the anharmonicity of the ν(XD) vibration is less than that of the ν(XH) and the mean-square amplitude of vibration is reduced.

The a_{mm} and b_{mm} each consist of two terms, which may be identified with the kinematic and the electronic coupling effects respectively. The expectation value of $e^{\alpha\gamma(r-r_0)}$ will depend primarily on the anharmonicity of the ν(XH) motion, since the leading term in the expansion of $(e^{\alpha\gamma(r-r_0)}-1)$ is odd, and it follows that deuteration will reduce the kinematic coupling. The expectation value of $(e^{-\beta(r-r_0)}-1)^2$ is, to first approximation, proportional to the mean-square amplitude of the ν(XH) vibration, and thus the electronic coupling effect is also reduced by deuteration. The net result is that the displacement $|s_{11}-s_{00}|$ between the minima of $U_{00}(s)$ and $U_{11}(s)$ is reduced by deuteration, and this will result in diminished Franck–Condon factors for $|0,n\rangle \rightarrow |1,n\pm1\rangle$ transitions, and in altered rotational profiles.

This is illustrated in table 4, where the term values and intensities of transitions in $Me_2O.DCl$ are presented. As before, the intensities have been normalized so that the sub-band corresponding to $\Delta n = 1$ has a total strength of unity. However, the sub-band corresponding to $\Delta n = 0$, centred at 1800 cm^{-1}, is now found to be the most intense. The central peak of the experimental spectrum is at 1850 cm^{-1} (Bertie & Falk 1973); the discrepancy between these values suggests that the chosen representation of the potential energy surface may somewhat underestimate the anharmonicity of the ν(XH) motion.

TABLE 3. THE EFFECT OF DEUTERATION ON THE EFFECTIVE POTENTIALS

parameter	$Me_2O.DCl$	$MeO_2.HCl$
τ	56.3	55.9
a_{00}	0.998	0.998
b_{00}	0.949	0.932
a_{11}	0.995	0.996
b_{11}	0.853	0.805
q_0	57.7	57.8
q_1	60.7	62.0
$(s_{00}-s_0)$/pm	−4.8	−6.6
$(s_{11}-s_0)$/pm	−14.9	−20.6
D_{00}/cm^{-1}	2888	2940
D_{11}/cm^{-1}	3197	3383

A reconstruction of the $Me_2O.DCl$ spectrum is shown in figure 8. This is not in very satisfactory agreement with experiment: the observed spectrum has shoulders at 50 cm^{-1} to each side of the central peak, while the weaker features further away cannot be resolved. As in the case of the $Me_2O.HCl$ species, it is impossible to understand the details of the spectrum in terms of ν(XH) $\pm n\nu$(XH..Y) transitions and vibration–rotation coupling alone, and the most natural explanation of the discrepancies between theory and experiment seems to be that combinations involving hydrogen bond bending modes contribute significantly to what is observed (Bertie & Falk 1973).

4.2. *The connection with the Ubbelohde effect*

The results of the preceding section show that the minimum position s_{00} of the effective potential $U_{00}(s)$ governing the ν(XH..Y) vibration in the ν(XH) ground state is sensitive to deuteration: $(s_{00} - s_0)$ is −6.6 pm for the $Me_2O.HCl$ species but only −4.8 pm for its deuterated analogue. The reason for this is very simple: both the coupling mechanisms depend critically on the vibrational amplitude of the proton or deuteron, and that of the latter is smaller.

It has been observed by Sheppard (1959) that there is a close connection between the tendency for the minima of the effective potentials to be displaced towards smaller values of the coordinate with increasing strength of coupling between the vibrational modes, and the tendency of the lattice constants of hydrogen-bonded crystals to increase on deuteration; and that the explanation of the Ubbelohde effect advanced by Gallagher (1959) may be interpreted in this way. Although in many instances the expansion following deuterium substitution in crystals is not entirely localized in the hydrogen bond (Delaplane & Ibers 1966; Hamilton & Ibers 1968), so that results obtained for isolated complexes are not necessarily a reliable guide to the behaviour of solids, it is nevertheless of considerable interest to explore Sheppard's suggestion in detail for the $Me_2O.HCl$ complex.

Since the Ubbelohde effect is believed to be primarily a zero-point rather than a thermal effect

(Gallagher 1959), the problem is simply to calculate the ground state expectation value $\langle XY\rangle$ of the X..Y distance for each isotopic analogue. From (2.1.1) it follows that in either case

$$\langle XY\rangle = \langle s\rangle + (1-\gamma)\langle r\rangle. \tag{4.2.1}$$

The expectation values of $(s-s_0)$ and $(r-r_0)$ can be calculated without difficulty from the wavefunctions of (2.2.4) and (2.3.4). However, it must be borne in mind that s_0 changes on deuteration. Since r_0 and R_0, the XH and H..Y separations at the global minimum of the potential energy surface, are expected to be independent of m_H, it is apparent from (2.1.1) and (2.1.2) that s_0 will depend somewhat on m_H through the mass ratio γ.

From (2.2.1) and (2.2.4) it follows that

$$\begin{aligned}\langle s-s_0\rangle &= -\alpha^{-1}\langle \ln z\rangle \\ &= -\alpha^{-2}N_{00}^2\int_0^\infty z^{-2}\{M_{q_0,\,q_0-\frac{1}{2}}(2\tau b_{00}^{\frac{1}{2}}z)\}^2\ln z\,dz.\end{aligned} \tag{4.2.2}$$

TABLE 4. CALCULATED VIBRATIONAL TERM VALUES AND INTENSITIES FOR $Me_2O.DCl$ AT 300 K

transition	term values / cm^{-1}	Franck–Condon factor	intensity	sub-band intensity
$\|0,1\rangle \rightarrow \|1,0\rangle$	1703.5	0.214	0.147	
$\|0,2\rangle \rightarrow \|1,1\rangle$	1710.5	0.271	0.118	
$\|0,3\rangle \rightarrow \|1,2\rangle$	1717.4	0.247	0.068	
$\|0,4\rangle \rightarrow \|1,3\rangle$	1724.4	0.190	0.034	
$\|0,5\rangle \rightarrow \|1,4\rangle$	1731.3	0.126	0.014	0.39
$\|0,6\rangle \rightarrow \|1,5\rangle$	1738.3	0.072	0.005	
$\|0,7\rangle \rightarrow \|1,6\rangle$	1745.2	0.033	0.002	
$\|0,8\rangle \rightarrow \|1,7\rangle$	1752.1	0.009	0.000	
$\|0,9\rangle \rightarrow \|1,8\rangle$	1759.1	0.001	0.000	
$\|0,0\rangle \rightarrow \|1,0\rangle$	1801.8	0.724	0.797	
$\|0,1\rangle \rightarrow \|1,1\rangle$	1807.1	0.335	0.231	
$\|0,2\rangle \rightarrow \|1,2\rangle$	1812.3	0.124	0.054	
$\|0,3\rangle \rightarrow \|1,3\rangle$	1817.5	0.027	0.008	
$\|0,4\rangle \rightarrow \|1,4\rangle$	1822.7	0.000	0.000	1.10
$\|0,5\rangle \rightarrow \|1,5\rangle$	1827.9	0.011	0.001	
$\|0,6\rangle \rightarrow \|1,6\rangle$	1833.1	0.039	0.003	
$\|0,7\rangle \rightarrow \|1,7\rangle$	1838.3	0.072	0.004	
$\|0,8\rangle \rightarrow \|1,8\rangle$	1843.5	0.102	0.003	
$\|0,0\rangle \rightarrow \|1,1\rangle$	1905.4	0.251	0.276	
$\|0,1\rangle \rightarrow \|1,2\rangle$	1908.9	0.384	0.264	
$\|0,2\rangle \rightarrow \|1,3\rangle$	1912.3	0.437	0.190	
$\|0,3\rangle \rightarrow \|1,4\rangle$	1915.8	0.436	0.120	
$\|0,4\rangle \rightarrow \|1,5\rangle$	1919.3	0.402	0.071	1.00
$\|0,5\rangle \rightarrow \|1,6\rangle$	1922.8	0.350	0.040	
$\|0,6\rangle \rightarrow \|1,7\rangle$	1926.2	0.290	0.022	
$\|0,7\rangle \rightarrow \|1,8\rangle$	1929.7	0.230	0.011	
$\|0,8\rangle \rightarrow \|1,9\rangle$	1933.2	0.170	0.006	
$\|0,0\rangle \rightarrow \|1,2\rangle$	2007.2	0.025	0.027	
$\|0,1\rangle \rightarrow \|1,3\rangle$	2008.9	0.065	0.045	
$\|0,2\rangle \rightarrow \|1,4\rangle$	2010.7	0.114	0.049	
$\|0,3\rangle \rightarrow \|1,5\rangle$	2012.4	0.166	0.046	
$\|0,4\rangle \rightarrow \|1,6\rangle$	2014.1	0.219	0.039	0.30
$\|0,5\rangle \rightarrow \|1,7\rangle$	2015.9	0.269	0.031	
$\|0,6\rangle \rightarrow \|1,8\rangle$	2017.6	0.314	0.023	
$\|0,7\rangle \rightarrow \|1,9\rangle$	2019.4	0.353	0.017	
$\|0,8\rangle \rightarrow \|1,10\rangle$	2021.1	0.645	0.021	

PHILOSOPHICAL TRANSACTIONS OF THE ROYAL SOCIETY A MATHEMATICAL, PHYSICAL & ENGINEERING SCIENCES

It is simpler to use an integration variable defined by

$$x = 2\tau b_{00}^{\frac{1}{2}} z. \tag{4.2.3}$$

On substitution into (4.4.2) of the expressions for N_{00}^2 and $M_{q_0, q_0-\frac{1}{2}}(x)$ given in equations (2.2.19) and (2.2.15) of II, it is found that

$$\langle s - s_0 \rangle = -\alpha^{-1}\Gamma(2q_0 - 1)\int_0^\infty [x^{2q_0-2} \ln x \, e^{-x}]\, dx + \alpha^{-1} \ln (2\tau b_{00}^{\frac{1}{2}}). \tag{4.2.4}$$

The integral is in a standard form, and is equal to $(2q_0 - 1)\,\psi(2q_0 - 1)$, where ψ denotes the logarithmic derivative of the gamma function (Abramovitz & Stegun 1964). After some rearrangement, and the use of (2.2.3), the expression becomes

$$\langle s \rangle = s_0 + \alpha^{-1} \ln (b_{00}/a_{00}) + \alpha^{-1}[\ln (2q_0) - \psi(2q_0 - 1)]. \tag{4.2.5}$$

The equation can easily be interpreted. From (2.1.20), the sum of the first two terms is simply s_{00}, the position of the minimum of $U_{00}(s)$. The third term is a correction for the anharmonicity of the hydrogen bond vibration.

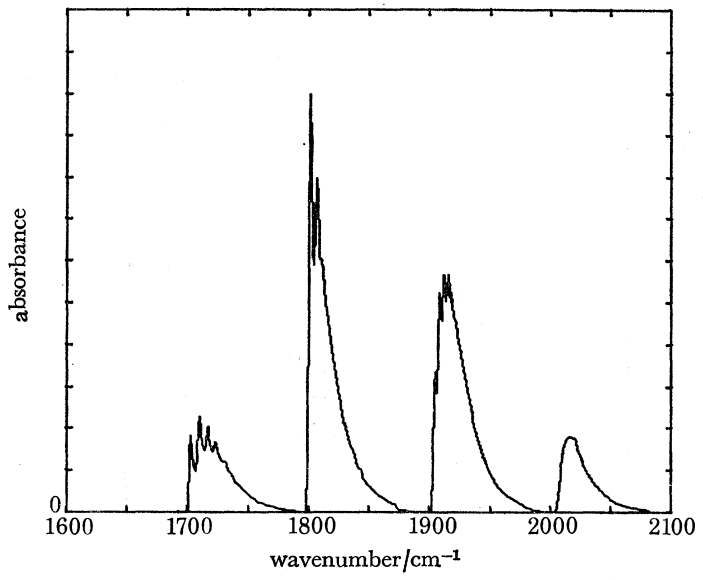

FIGURE 8. The calculated profile of the ν(XD) absorption band in $Me_2O.DCl$.

A very similar analysis shows that

$$\langle r \rangle = r_0 + \beta^{-1}[\ln (2\tilde{k}) - \psi(2\tilde{k} - 1)], \tag{4.2.6}$$

where the second term is a correction for the ν(XH) anharmonicity. From (4.2.1) the average X..Y distance is given by

$$\langle \mathrm{XY} \rangle = s_0 + (1 - \gamma)\, r_0 + \alpha^{-1} \ln (b_{00}/a_{00}) + \alpha^{-1}[\ln (2q_0) - \psi(2q_0 - 1)] + (1 - \gamma)\, \beta^{-1}[\ln (2\tilde{k}) - \psi(2\tilde{k} - 1)]. \tag{4.2.7}$$

The sum of the first two terms is simply $r_0 + R_0$, which is invariant under isotopic substitution. The remaining three terms all depend to some extent on m_{H}, and must be considered in turn.

The term $\alpha^{-1} \ln (b_{00}/a_{00})$, representing the displacement $(s_{00} - s_0)$ of the minimum of $U_{00}(s)$, has already been evaluated; the displacement towards smaller values of the coordinate is greater

by 1.8 pm in the protium than in the deuterium species, so that this term tends to increase the $\langle XY\rangle$ separation on deuteration.

The anharmonicity correction $\alpha^{-1}[\ln(2q_0)-\psi(2q_0-1)]$ for the $\nu(XH..Y)$ motion is not particularly sensitive to isotopic substitution, since the shape of the potential well $U_{00}(s)$, and thus the value of the parameter q_0, depends little on m_H. From the recurrence relation

$$\psi(z+1) = \psi(z) + z^{-1} \tag{4.2.8}$$

and the asymptotic expansion

$$\psi(z) \sim \ln z - \frac{1}{2z} - \sum_{n=1}\left(\frac{B_{2n}}{2n\,z^{2n}}\right), \tag{4.2.9}$$

where the B_{2n} are Bernoulli numbers (Abramovitz & Stegun 1964), it is easy to evaluate the correction: it is found that

$$\alpha^{-1}[\ln(2q_0) - \psi(2q_0-1)] = 0.75\,(\alpha q_0)^{-1} + O(q_0^{-2}). \tag{4.2.10}$$

The correction is thus 1.61 pm for the protium and barely 0.01 pm less for the deuterium species; the change it produces on deuteration is two orders of magnitude smaller than that produced by the displacement of the minima, and can be ignored.

The term $(1-\gamma)\,\beta^{-1}[\ln(2\tilde{k}) - \psi(2\tilde{k}-1)]$, representing a correction for $\nu(XH)$ anharmonicity, can be evaluated in essentially the same way: to first approximation the correction is $0.75\,(1-\gamma)\,(\beta\tilde{k})^{-1}$. The parameter $\tilde{k}$ is proportional to $\mu_1^{\frac{1}{2}}$, so that $\langle r-r_0\rangle$ has a similar mass dependence and decreases from 1.7 pm to 1.2 pm on deuteration. However, because of the factor $(1-\gamma)$, this has very little effect on the $\langle XY\rangle$ distance: $(1-\gamma)\,\langle r-r_0\rangle$ increases from 0.05 pm to 0.07 pm on deuteration. The point is that the centre of mass of the XH molecule is necessarily close to the X atom, so that any decrease in $\langle r\rangle$ due to a decreased vibrational amplitude in an anharmonic potential has little effect on the mean distance between the X atom and XH centre of mass. The principal consequence of a decreased $\nu(XH)$ vibrational amplitude is a reduction in the coupling between the $\nu(XH)$ and $\nu(XH..Y)$ modes, and this affects the mean distance between the XH centre of mass and the Y atom.

It is clear, therefore, that of the five terms in equation (4.2.7) the third, describing the displacement of the minimum of $U_{00}(s)$ due to the anharmonic coupling between the vibrational modes, is by far the most sensitive to deuterium substitution, and must be responsible for the Ubbelohde effect. However, it is possible to distinguish between two coupling mechanisms, the kinematic and the electronic, acting in opposite senses, which have been combined in the definition of the parameters a_{00} and b_{00} determining the displacement. In order to obtain some insight into the trends which are observed experimentally it is useful to consider the contribution of each mechanism separately.

The hypothetical values of $\alpha^{-1}\ln(b_{00}/a_{00})$ which would apply in the absence of any electronic coupling can be obtained by setting $c_1 = c_2 = 0$ in (2.3.10) and (2.3.11), noting that this also affects the definition of $\tilde{k}$ through (2.3.2) and (2.3.5). The results of II are then regained†, namely that $\langle s_{00} - s_0\rangle$ is $+2.7$ pm for $Me_2O.HCl$ and $+1.9$ pm for $Me_2O.DCl$. The effect of kinematic coupling alone would therefore be to produce a contraction of about 0.8 pm on deuteration. This figure is not particularly sensitive to the strength of hydrogen bonding, as measured by D_2, although it does depend on the anharmonicity of the $\nu(XH)$ mode. Thus the above hypothetical estimate of the contraction which would be produced on deuteration if the $\nu(XH)$ vibration were

† The slight numerical discrepancy between the results quoted here and those of table 6 of II is due to the different value assumed for the $\nu(XH..Y)$ frequency in that paper.

unaffected by hydrogen bond formation (i.e. if the term $V_3(r,s)$ in (2.1.3) were to vanish) is probably representative of quite a wide variety of hydrogen-bonded systems of moderate strength.

The isotope dependence of the electronic coupling effect is critically sensitive to the values of the parameters c_1 and c_2 used to represent the potential energy surface. A rough estimate of the displacement of the minimum of $U_{00}(s)$ resulting from electronic coupling alone can be obtained by setting the first terms in (2.3.10) and (2.3.11) equal to unity and expanding $\alpha^{-1}\ln(b_{00}/a_{00})$. To first approximation the displacement of the minimum is then given by $(c_2+\frac{1}{2}c_1)D_1/2\alpha\tilde{k}D_2$. On deuteration the parameter $\tilde{k}$ increases by some 40 %, so that the magnitude of the displacement is reduced; however, the sign of the displacement is determined by that of $(c_2+\frac{1}{2}c_1)$. In the case of $Me_2O.HCl$ this term is dominated by the large negative value found for c_2, and the contribution to the displacement is found to be -9.3 pm for the protium and -6.7 pm for the deuterium species, so that electronic coupling alone would produce an expansion of 2.6 pm on deuteration, a much larger effect than the contraction which would be produced by kinematic coupling alone. In practice the two effects interfere (though they are not exactly additive), and it is predicted that the Cl...O distance should be 1.8 pm greater in $Me_2O.DCl$ than in $Me_2O.HCl$.

The factor $(c_1+\frac{1}{2}c_2)$, to which the electronic coupling contribution to the Ubbelohde effect is roughly proportional, is very closely related to the fractional shift in the ν(XH) absorption frequency produced by hydrogen bond formation, which is given to first approximation by $[(1+c_1+c_2)^{\frac{1}{2}}-1]$. Provided that the downward frequency shift is sufficiently large, so that electronic coupling outweighs kinematic, there should be a strong correlation between frequency shift and Ubbelohde expansion. If the hydrogen bonding is weak and the frequency shift small, kinematic coupling may dominate, in which case deuterium substitution may result in a small contraction of the system. If the hydrogen bonding is very strong, however, and the proton moves in a symmetrical or nearly symmetrical potential, no conclusions can be drawn, since the present model is not applicable. This latter case has been treated theoretically by Singh & Wood (1969).

Gallagher (1959) has argued, solely from experimental considerations, that the overall isotopic expansion must be the sum of two terms which act in opposite senses. The present interpretation of the Ubbelohde effect is in complete agreement with this idea, and shows the origin of the two opposing mechanisms. Furthermore, it gives mathematical expression to the argument of Sheppard (1959), that the minimum of the potential curve for the ν(XH..Y) vibration will lie at a smaller value of the coordinate than that of the ν(XD..Y) vibration, owing to the coupling between the two stretching modes being dependent on the ν(XH) vibrational amplitude.

It should be observed that the present argument makes no appeal to the existence of a subsidiary minimum in the potential function for the proton at fixed X..Y separation (cf. figure 2). While these calculations in no way prejudice the possible existence of asymmetric double minimum potentials in hydrogen-bonded systems, they do show that there is no necessary connection between such potentials and an expansion of the system on deuteration.†

Finally, it should be remarked that the predicted expansion of $Me_2O.HCl$ on deuteration is very

† The theoretical study by Singh & Wood (1969) has sometimes been interpreted as showing that a hydrogen-bonded system will expand on deuteration only if the proton potential has two minima. Singh & Wood themselves very properly emphasise that their results are only applicable to a symmetric (XHX) system, possibly with a small asymmetric perturbation in the potential. Thus the type of situation they envisage is necessarily rather different from the case considered here, and any conflict is more apparent than real. Indeed, the present interpretation of Gallagher's expansion term is similar to theirs.

PHILOSOPHICAL TRANSACTIONS OF THE ROYAL SOCIETY A MATHEMATICAL, PHYSICAL & ENGINEERING SCIENCES

similar in magnitude to that predicted for the $(HCOOH)_2$ dimer by Y. Maréchal (1972), which is in good agreement with the experimental result of Almenningen, Bastiansen & Motzfeldt (1970).

5. Conclusions and summary

The theory of the anharmonic coupling between ν(XH) and ν(XH..Y) vibrational modes developed previously (Coulson & Robertson 1975) assumed pairwise additive interactions between the X, H and Y atoms, and the model potential energy surface was insufficiently refined to reproduce spectroscopic phenomena accurately. In the present paper the theory has been generalized so as to accommodate a much more realistic class of potential function, which allows for the effect of varying hydrogen bond length on the electron distribution in the XH region. By taking advantage of the extensive information available about the temperature dependence of the Me_2O.HCl spectrum it has been possible to determine the additional parameters needed to specify the potential in that particular case.

The availability of a reasonably detailed potential energy surface allows a substantial number of conclusions to be drawn. It is found that the electronic coupling acts in the opposite sense to the kinematic coupling mechanism, and outweighs it, so that the effective potential curve for the ν(XH..Y) motion is progressively displaced towards smaller values of the coordinate as the amplitude of the ν(XH) vibration increases. In particular, the complex is predicted to be 14 pm shorter in its first excited ν(XH) state than in the ground state.

The effect on the vibration–rotation band profiles is spectacular: each $|0, n_0\rangle \rightarrow |1, n_1\rangle$ transition is expected to give rise to a severely distorted vibration–rotation band with a pronounced P branch band head and a long, sloping R branch. This is in satisfactory agreement with the conclusions of Thomas & Thompson (1970) regarding the shape of the rotational bands of the CH_3CN.HCl species. In the present case the effect on the rotational bands is expected to be more pronounced than in the case investigated by Thomas & Thompson, but this is entirely reasonable, since there is no clear evidence for the formation of ν(XH) $\pm n\nu$(XH..Y) combination bands in CH_3CN.HCl, which suggests that the shortening of the first ν(XH) excited state of Me_2O.HCl should be more pronounced than that of CH_3CN.HCl.

Isotopic substitution reduces the ν(XH) vibrational amplitude, and thus the displacement of the minimum of each ν(XD..Y) effective potential curve is less marked than that of the corresponding ν(XH..Y) curve. The Franck–Condon factors for $|0, n\rangle \rightarrow |1, n \pm 1\rangle$ transitions, which depend critically on the extent to which the two curves are staggered, are reduced in consequence. This gives at least a qualitative account of the sensitivity of the Me_2O.HCl spectrum to deuteration. To a very good approximation the change in the mean X..Y separation produced by deuterium substitution can be understood in terms of the change in position of the minimum of the ground state effective potential curve, as envisaged by Sheppard (1959). The mean O..Cl separation is predicted to be 1.8 pm greater in Me_2O.DCl than in Me_2O.HCl, and as this figure is expected to be rather sensitive to the finer details of the potential energy surface, an experimental measurement of the isotope effect ought to provide valuable information about the electronic coupling mechanism.

In view of the finding that the potential curves for Me_2O.HCl intersect, the question of vibrational predissociation treated in I must be re-examined. Since the intersection is rather oblique, and lies high up on the repulsive portions of the curves, which is precisely where they are least reliable, the position of the crossing point is not accurately determined and the calculated values

PHILOSOPHICAL TRANSACTIONS OF THE ROYAL SOCIETY A MATHEMATICAL, PHYSICAL & ENGINEERING SCIENCES

($s_{\text{cross}} - s_0 = -103$ pm; $E_{\text{cross}} = 5860$ cm^{-1}) must not be taken too seriously. Nevertheless, the finding that the crossing point lies above the horizontal asymptote of $U_{11}(s)$ (at 2910 cm^{-1})† is important: it means that the classical turning point of any quasi-stationary $|1, n\rangle$ state lies at lower energy than the crossing point, so that the radiationless decay of the state involves tunnelling through a potential barrier. This excludes any possibility of very rapid predissociation (on a time-scale comparable with a ν(XH..Y) quarter-period). However, the potential barrier is narrow just below the crossing point, and very highly excited $|1, n_1\rangle$ states, with energies close to the $U_{11}(s)$ dissociation limit (i.e. with $n + \frac{1}{2}$ not much smaller than q_1, cf. equation 2.2.16 of II) may well have appreciable widths, many orders of magnitude greater than the estimates of I. On the other hand, the barriers to predissociation of $|1, n_1\rangle$ states with $n_1 \leqslant 10$ are very broad, and there is no reason to suppose that predissociative broadening should be observable. Indeed, predissociation of $|1, n_1\rangle$ states with $n_1 \leqslant 4$ is energetically impossible, since a portion of the $U_{11}(s)$ curve lies below the horizontal asymptote of $U_{00}(s)$.‡ Although the calculations of I clearly need revision, the main conclusion of that paper, that predissociation fails to contribute significantly to the observed spectral broadening, remains secure.

It is interesting to note that the potential curve $U_{00}(s)$ has a depth D_{00} of 2940 cm^{-1} (cf. table 2) whereas the quantity D_2, which we have referred to somewhat loosely as the hydrogen bond dissociation energy, is only 2750 cm^{-1}. The discrepancy can to a great extent be understood in terms of the altered zero point energy of the ν(XH) mode following hydrogen bond formation; the ν(XH) zero point energy, including anharmonicity corrections, is 1482 cm^{-1} for free HCl but only 1297 cm^{-1} in the Me_2O.HCl complex. In order to increase s from s_0 to infinity work must be done to increase the ν(XH) zero point energy. The depth D_{00} of $U_{00}(s)$, which represents the binding energy of the hydrogen bond, is thus expected to be some 185 cm^{-1} greater than D_2. The calculated difference is 190 cm^{-1}. It should be observed that D_2 is not an experimentally measurable quantity, but refers to the depth of the potential energy surface minimum $V(r_0, s_0)$ relative to $V(r_0, \infty)$.

The value of D_{00} for the Me_2O.DCl species is 2888 cm^{-1} (cf. table 3), so that the deuterium bond is weaker by 52 cm^{-1} or 0.0065 eV than the corresponding hydrogen bond. Again, the difference can be understood in terms of changes in zero point energy. Similar conclusions have been reached by Y. Maréchal (1972) in connection with the $(HCOOH)_2$ dimer.

Although suggestive in many ways, these calculations do not give a satisfactory account of the overall ν(XH) band shapes of either the Me_2O.HCl or the Me_2O.DCl species, as they fail to account for the merging of the sub-bands and predict a fine structure which is not observed. Since one of the critical parameters has been estimated by comparing the temperature dependence of experimental spectra with theoretical reconstructions, and the agreement obtained is only qualitatively correct, it is right to ask whether the various positive conclusions that have been drawn are in any way jeopardized by this lack of detailed agreement. Two main questions arise: first, whether the procedure used to determine the parameters c_1 and c_2 in the assumed potential function (2.1.3) is adequate; and secondly, whether the special form assumed for the potential function is sufficiently flexible to describe the two coupled vibrational modes satisfactorily.

† This asymptote should really lie at 2885 cm^{-1}; in assuming an approximate wavefunction of the form (2.1.11) and neglecting the dependence of $\chi(r)$ on the coordinate s an error is introduced which becomes more pronounced as s increases. The error in $U_{11}(s)$ is of the order of 1%, which is perfectly acceptable.

‡ This finding is critically dependent on the value of the hydrogen bond dissociation energy, which is difficult to determine accurately from experiment (Seel 1966). Furthermore, the quantity determined by Seel cannot be precisely identified with the parameter D_2 defined in (2.1.5).

PHILOSOPHICAL TRANSACTIONS OF THE ROYAL SOCIETY A MATHEMATICAL, PHYSICAL & ENGINEERING SCIENCES

Electrical anharmonicity and the formation of combinations with hydrogen bond bending modes may each be expected to influence the spectrum, and thus to complicate the procedure for determining the parameters c_1 and c_2. It was shown in II that the two dominant terms in the transition dipole

$$\langle 1, n_1 | \mu(r, s) | 0, n_0 \rangle$$

are likely to be $$(\partial\mu/\partial r)_{r_0 s_0} \langle 1, n_1 | (r - r_0) | 0, n_0 \rangle$$

and $$(\partial^2\mu/\partial r \partial s)_{r_0 s_0} \langle 1, n_1 | (r - r_0)(s - s_0) | 0, n_0 \rangle.$$

The present analysis has been based on the assumption that the second term is much smaller than the first, and the potential energy surface has been determined by requiring that the products of Franck–Condon factors $|\langle n_1 | n_0 \rangle|^2$ with the appropriate Boltzmann factors, when summed, reproduce the temperature dependence of the spectrum. If electrical anharmonicity is significant, our estimate of the pattern of Franck–Condon factors, and hence of the separation between the minima of the effective potentials $U_{00}(s)$ and $U_{11}(s)$, will be in error, and this will tend to vitiate the remainder of the analysis. For this reason an accurate calculation of the dipole moment surface for the complex would be most valuable.

A correction for electrical anharmonicity will not affect the position of vibrational terms, unless by any chance the present calculations grossly underestimate the difference in curvature between the upper and lower effective potentials, which is rather unlikely. To account for the merging of the vibrational sub-bands it seems necessary to suppose that combination bands $\nu(\mathrm{XH}) \pm n\nu(\mathrm{XH}..\mathrm{Y}) \pm n'\delta(\mathrm{XH}..\mathrm{Y})$, involving low frequency bending modes of the hydrogen bond, are excited. Bertie & Falk (1973) conclude that the $\delta(\mathrm{XH}..\mathrm{Y})$ frequency is about 50 cm^{-1}, or roughly half the $\nu(\mathrm{XH}..\mathrm{Y})$ frequency.† This raises a distinct possibility of appreciable overlapping between bands such as

$$\nu(\mathrm{XH}) + \delta(\mathrm{XH}..\mathrm{Y})$$

and $$\nu(\mathrm{XH}) + \nu(\mathrm{XH}..\mathrm{Y}) - \delta(\mathrm{XH}..\mathrm{Y}),$$

which would render our procedure for estimating coupling parameters very dubious.

The question whether a function of the form (2.1.3) is sufficiently flexible to represent the true potential energy surface is difficult to answer. Clearly there are certain well-established phenomena, such as the increase in the equilibrium value of the XH coordinate with decreasing X..Y separation, which are not reproduced at all by such a function; whether this is of any spectroscopic importance is a matter for speculation. In the last resort, the question can only be resolved by undertaking extensive electronic structure calculations and seeing whether the general features of the calculated potential energy surface can be reproduced by (2.1.3); detailed agreement is hardly to be expected. Nevertheless, it seems very likely that the potential energy surface used in this paper is sufficiently accurate to capture many of the essential features of the problem; its principal merit lies not in any claim to represent the true potential with great precision, but rather in its relative simplicity, which enables the analysis of the coupling between anharmonic modes to be performed algebraically rather than numerically, and has the valuable advantage that mechanisms responsible for particular phenomena can be discerned.

† The $\delta(\mathrm{XH}..\mathrm{Y})$ frequency has been much more accurately determined for the $CH_3CN.HF$ complex by Thomas (1971*b*), who finds a value of 40 cm^{-1}.

PHILOSOPHICAL TRANSACTIONS OF THE ROYAL SOCIETY A MATHEMATICAL, PHYSICAL & ENGINEERING SCIENCES

I wish to thank Dr R. M. Seel for permission to make use of unpublished experimental results, and Professor N. Sheppard, F.R.S., for much helpful advice.

MM. Bouteiller and E. Maréchal have independently shown that the temperature dependence of the $Me_2O.HCl$ spectrum can be understood in terms of a rather simpler model which neglects the anharmonicity of the ν(XH..Y) vibration; I am grateful to them for sending me a copy of their paper prior to publication, and for discussions.

Appendix A

It is necessary to evaluate the parameters a_{mm} and b_{mm} of (2.1.18) and (2.1.19) and the level shifts $\Delta\epsilon_m$ of (2.1.15).

The normalized wavefunction $\chi_m(r)$ of (2.3.4) can be expressed in terms of Kummer's function as

$$\chi_m(r) = N_m \mathrm{e}^{-\frac{1}{2}\zeta}\zeta^{k-m-\frac{1}{2}}{}_1F_1(-m; 2\tilde{k}-2m; \zeta), \tag{A 1}$$

where

$$N_m^2 = \frac{\beta\Gamma(2\tilde{k}-m)}{m!\,\Gamma(2\tilde{k}-2m-1)\,\Gamma(2\tilde{k}-2m)}. \tag{A 2}$$

The parameters a_{mm} and b_{mm} are defined as follows:

$$a_{mm} = \int_0^\infty \chi_m^2(r)\left\{\exp\alpha\gamma(r-r_0) - \left(\frac{c_1 D_1}{2D_2}\right)(1-\exp(-(r-r_0)))^2\right\}\mathrm{d}r \tag{A 3}$$

and

$$b_{mm} = \int_0^\infty \chi_m^2(r)\left\{\exp 2\alpha\gamma(r-r_0) + \left(\frac{c_2 D_1}{D_2}\right)(1-\exp(-\beta(r-r_0)))^2\right\}\mathrm{d}r. \tag{A 4}$$

Thus

$$\begin{aligned} a_{00} &= N_0\int_0^\infty \mathrm{d}\zeta(\beta\zeta)^{-1}(\mathrm{e}^{-\frac{1}{2}\zeta}\zeta^{\tilde{k}-\frac{1}{2}})^2\left[(\zeta/2\tilde{k})^{-\eta} - \left(\frac{c_1 D_1}{2D_2}\right)(1-\zeta/2\tilde{k})^2\right] \\ &= \frac{(2\tilde{k})^\eta}{\Gamma(2\tilde{k}-1)}\int_0^\infty \mathrm{e}^{-\zeta}\zeta^{2\tilde{k}-2-\eta}\,\mathrm{d}\zeta - \frac{c_1 D_1}{2D_2\,\Gamma(2\tilde{k}-1)}\int_0^\infty \mathrm{e}^{-\zeta}\zeta^{2\tilde{k}-2}[1-\zeta/\tilde{k}+\zeta^2/4\tilde{k}^2]\,\mathrm{d}\zeta, \end{aligned} \tag{A 5}$$

where

$$\eta = \alpha\gamma/\beta. \tag{A 6}$$

The result of (2.3.10) follows immediately, and the expressions quoted for b_{00}, a_{11} and b_{11} can be obtained in the same way.

The level shifts $\Delta\epsilon_m$ are given by

$$\begin{aligned} \Delta\epsilon_m &= -\int_0^\infty \chi_m^2(r)\,V_3(r, s_0)\,\mathrm{d}r \\ &= -D_1(c_1+c_2)\int_0^\infty \chi_m^2(r)\,[1-\exp(-\beta(r-r_0))]^2\,\mathrm{d}r. \end{aligned} \tag{A 7}$$

Thus

$$\Delta\epsilon_0 = -\frac{D_1(c_1+c_2)}{\Gamma(2\tilde{k}-1)}\int_0^\infty \mathrm{e}^{-\zeta}\zeta^{2\tilde{k}-2}(1-\zeta/2\tilde{k})^2\,\mathrm{d}\zeta, \tag{A 8}$$

from which the result of (2.3.8) is easily obtained. The result quoted for $\Delta\epsilon_1$ follows in the same way.

References

Abramovitz, M. & Stegun, I. A. 1964 *Handbook of mathematical functions*. Washington D.C.: National Bureau of Standards.

Almenningen, A., Bastiansen, O. & Motzfeldt, T. 1970 *Acta Chem. Scand.* **24**, 747.

Belozerskaya, L. P. & Shchepkin, D. N. 1966 *Optics Spectrosc.* Suppl. II, 146.

Bertie, J. E. & Falk, M. V. 1973 *Can. J. Chem.* **51**, 1713.

Bertie, J. E. & Millen, D. J. 1965 *J. chem. Soc.* 497, 514.

Bouteiller, Y. & Maréchal, E. 1975 *C. r. hebd. Séanc. Acad. Sci., Paris* B **220**, 5.

Coulson, C. A. & Robertson, G. N. 1974 *Proc. R. Soc. Lond.* A **337**, 167.

Coulson, C. A. & Robertson, G. N. 1975 *Proc. R. Soc. Lond.* A **342**, 289.

Delaplane, R. G. & Ibers, J. A. 1966 *J. chem. Phys.* **45**, 3451.

Gallagher, K. J. 1959 *Hydrogen bonding* (ed. D. Hadzi). London: Pergamon.

Hamilton, W. C. & Ibers, J. A. 1968 *Hydrogen bonding in solids*. New York: Benjamin.

Herzberg, G. 1950 *Spectra of diatomic molecules*. Princeton: van Nostrand.

Lascombe, J., Lassègues, J.-C. & Huong, P. V. 1973 *J. phys. Chem.* **27**, 991.

Lassègues, J.-C. & Huong, P. V. 1972 *Chem. Phys. Lett.* **17**, 444.

Maréchal, E. & Bouteiller, Y. 1974 *C. r. hebd. Séanc. Acad. Sci. Paris* B **279**, 435.

Maréchal, Y. 1972 *Chem. Phys. Lett.* **13**, 237.

Powell, M. J. D. 1968 *A.E.R.E. Report*, no. R 5947. London: H.M.S.O.

Seel, R. M. 1966 Ph.D. Thesis, Cambridge.

Sheppard, N. 1959 *Hydrogen bonding* (ed. D. Hadzi). London: Pergamon.

Singh, T. & Wood, J. L. 1969 *J. chem. Phys.* **50**, 3572.

Slater, L. J. 1960 *The confluent hypergeometric function*. Cambridge University Press.

Thomas, R. K. & Thompson, H. W. 1970 *Proc. R. Soc. Lond.* A **316**, 303.

Thomas, R. K. 1971*a* *Proc. R. Soc. Lond.* A **322**, 137.

Thomas, R. K. 1971*b* *Proc. R. Soc. Lond.* A **325**, 133.

Ubbelohde, A. R. 1939 *Proc. R. Soc. Lond.* A **179**, 399.

Whittaker, E. T. & Watson, G. N. 1927 *Modern analysis*, 4th ed. Cambridge University Press.

Witkowski, A. & Maréchal, Y. 1968 *J. chem. Phys.* **48**, 3697.

PHILOSOPHICAL TRANSACTIONS OF THE ROYAL SOCIETY A MATHEMATICAL, PHYSICAL & ENGINEERING SCIENCES